NASA TECHNICAL NOTE

NASA TN D-3701

C.1

NASA TN D-3701

TRANSONIC AERODYNAMIC CHARACTERISTICS OF A MODEL OF A SUPERSONIC FIGHTER-BOMBER AIRPLANE WITH EXTERNAL FUEL TANKS AND OTHER MODIFICATIONS

by James C. Ferris

Langley Research Center
Langley Station, Hampton, Va.

NATIONAL AERONAUTICS AND SPACE ADMINISTRATION • WASHINGTON, D. C. • NOVEMBER 1966

TRANSONIC AERODYNAMIC CHARACTERISTICS OF A MODEL OF A SUPERSONIC FIGHTER-BOMBER AIRPLANE WITH EXTERNAL FUEL TANKS AND OTHER MODIFICATIONS

By James C. Ferris

Langley Research Center
Langley Station, Hampton, Va.

NATIONAL AERONAUTICS AND SPACE ADMINISTRATION

For sale by the Clearinghouse for Federal Scientific and Technical Information
Springfield, Virginia 22151 – Price $2.50

TRANSONIC AERODYNAMIC CHARACTERISTICS OF A MODEL OF A SUPERSONIC FIGHTER-BOMBER AIRPLANE WITH EXTERNAL FUEL TANKS AND OTHER MODIFICATIONS

By James C. Ferris
Langley Research Center

SUMMARY

An investigation was made of the static stability characteristics of a 1/22-scale model of a supersonic fighter-bomber airplane. The configurations included a short single-place model, a long two-place model, and models with external fuel tanks, a larger vertical tail, wing-leading-edge-flap deflections, and an afterbody fuel tank. The longitudinal aerodynamic characteristics were determined through an angle-of-attack range from -4° to 23° at an angle of sideslip of 0°, at Mach numbers from 0.60 to 1.20. The short model was also investigated through an angle-of-attack range from -12° to 30°, at a Mach number of 0.80, to determine the pitch-up characteristics of the model. The models were investigated through a sideslip range from -4° to 15° at fixed angles of attack of 0°, 5°, 10°, and 15°. All configurations were investigated with internal flow in the model.

The configurations were longitudinally stable through the normal angle-of-attack range; however, a pitch-up occurred at an angle of attack of 21° at a Mach number of 0.80 with the single-place model. The external fuel tanks caused a shift in trim to higher lift coefficients and substantial increases in drag.

The configurations were generally laterally stable, although substantial losses in directional stability occurred at high angles of attack. One configuration with a pylon-mounted fuel tank on the fuselage was directionally unstable at an angle of attack of 15.8° at Mach numbers of 0.90, 0.95, and 1.20.

INTRODUCTION

Wind-tunnel investigations at transonic and supersonic speeds have been made of the aerodynamic characteristics of single-place and two-place versions of a supersonic fighter-bomber airplane. The results of an investigation at supersonic speeds in the Langley Unitary Plan wind tunnel of the performance and the longitudinal and lateral static stability characteristics of both versions of this airplane are presented in reference 1. The performance and the longitudinal and lateral static stability characteristics

of both versions at transonic speeds obtained in the Langley 8-foot transonic tunnels are presented in references 2 and 3. Also included in references 2 and 3 is information on the effect on the longitudinal and lateral static stability characteristics of short and long body noses, external stores, an afterbody bump for fuel storage, and exit-nozzle blisters. Reference 4 presents the results of a supersonic wind-tunnel investigation of larger external fuel tanks, an afterbody bump for fuel storage, external bombs, a drooped fuselage forebody, extended wing tips, a larger vertical tail, and several designs of ventral fins. Presented in reference 5 are the results of a transonic wind-tunnel investigation to determine the effect of nose shape of flat-frontal-surface external stores on performance and static stability characteristics.

The purpose of the present investigation in the Langley 8-foot transonic pressure tunnel was to determine at transonic speeds the longitudinal and lateral static stability characteristics of a short single-place model, a long two-place model, 2.46-cubic-meter (650 U.S. gallon) external-fuselage and wing-pylon-mounted fuel tanks, a larger afterbody fuel tank, a larger vertical tail, and the effect of wing-leading-edge-flap deflection. The investigation was made through a Mach number range from 0.60 to 1.20.

SYMBOLS

The lift and drag data are referred to the wind and stability axes, the rolling-moment and yawing-moment data are referred to the body axes, and the lateral-force and pitching-moment data are referred to the common lateral axes of the stability axes and body axes. The origin of the stability and body axes was at the moment reference center located longitudinally at 25-percent mean aerodynamic chord of the wing and on the model reference line as shown in figure 1. All data presented herein were based on the planform dimensions of the wing.

The derivatives C_{L_α} and $C_{m_{C_L}}$ are for a lift coefficient of approximately zero. The derivatives C_{n_β}, C_{l_β}, and C_{Y_β} are for a sideslip angle of approximately 0^o.

The units used in the physical quantities in this paper are given both in the International System of Units (SI) and in the U.S. Customary Units. Details concerning the use of SI, together with physical constants and conversion factors, are given in reference 6.

b span (projected) of wing, meter (ft)

C_D wind axes external-drag coefficient, $\frac{\text{Wind-axis external drag}}{q_\infty S}$

C_{D}' stability-axis external-drag coefficient ($C_{D}' = -C_{X,S}$, where $C_{X,S}$ is external longitudinal-force coefficient along stability X-axis; also, $C_{D}' = C_{D}$ when $\beta = 0^{o}$), $\frac{\text{Stability-axis external drag}}{q_{\infty}S}$

$C_{D,i}$ internal drag coefficient

C_{L} lift coefficient, $\frac{\text{Lift}}{q_{\infty}S}$

C_{Y} lateral-force coefficient, $\frac{\text{Lateral force}}{q_{\infty}S}$

C_{l} rolling-moment coefficient, $\frac{\text{Rolling moment}}{q_{\infty}Sb}$

C_{m} pitching-moment coefficient, $\frac{\text{Pitching moment}}{q_{\infty}S\bar{c}}$

C_{n} yawing-moment coefficient, $\frac{\text{Yawing moment}}{q_{\infty}Sb}$

$\bar{c}$ mean aerodynamic chord of wing, $\frac{2}{3}c_{r}\frac{1+\lambda+\lambda^{2}}{1+\lambda}$

c_{t} nominal tip chord of wing, obtained by extending leading and trailing edges of wing to plane which is tangent to tip of wing, parallel to root chord of wing, and perpendicular to chord plane of wing

c_{r} root chord of wing, obtained by extending straight portions of leading and trailing edges of wing to plane of symmetry of model

L/D lift-drag ratio

M Mach number of undisturbed stream

q_{∞} dynamic pressure of undisturbed stream

R Reynolds number, based on $\bar{c}$

S area (projected) of wing, meter^2 (ft^2)

$\frac{w}{w_\infty}$ ratio of inlet mass flow to free-stream mass flow

α angle of attack, referred to the model reference line, deg

β angle of sideslip, deg

δ_h deflection of horizontal tail, determined by angle between plane of horizontal tail and reference line of body; positive when trailing edge is down, deg

δ_n deflection of leading-edge flap, determined by angle between chord plane of flap and chord plane of wing, measured in plane perpendicular to hinge line, positive when leading edge is up (fig. 1(b))

λ taper ratio of wing, $\frac{c_t}{c_r}$

$C_{L_\alpha} = \frac{\partial C_L}{\partial \alpha}$ per deg

$C_{m_{C_L}} = \frac{\partial C_m}{\partial C_L}$

$C_{n_\beta} = \frac{\partial C_n}{\partial \beta}$ per deg

$C_{l_\beta} = \frac{\partial C_l}{\partial \beta}$ per deg

$C_{Y_\beta} = \frac{\partial C_Y}{\partial \beta}$ per deg

Subscripts:

max maximum

min minimum

$(L/D)_{max}$ at maximum lift-drag ratio

APPARATUS

Tunnel

The investigation was made in the Langley 8-foot transonic pressure tunnel. The test section of this tunnel is square in cross section with slotted upper and lower walls to permit continuous operation through the transonic speed range. The total pressure of the tunnel air can be varied from a minimum value of about 0.25 atmosphere at all test Mach numbers to a maximum value of 2.0 atmospheres at Mach numbers up to 0.40 and about 1.5 atmospheres at transonic Mach numbers. The tunnel air is dried sufficiently to avoid condensation effects.

Models

The basic model used in the present investigation was a sting-supported 1/22-scale model of a supersonic fighter-bomber airplane. This airplane is turbojet powered and has wing-root air inlets. The wing and horizontal tail of the model had 45° of sweepback of the quarter-chord line. The vertical tail had 48° of sweepback of the leading edge. The airfoil sections (parallel to the body reference line and perpendicular to the chord plane) of the wing were NACA 65A005.5 at the 0.38 semispan station and NACA 65A003.7 at the tip, with a linear thickness variation between these stations. The model was built of steel and aluminum. Three-view drawings of the model with two fuselage lengths are shown in figure 1. The horizontal-tail deflection was -3°, and a leading-edge-flap deflection of -7.5 was used for most configurations. The model inlets and duct were designed for internal flow. Supersonic wing-root inlets were included on the model, and boundary-layer diverters were used with the inlets. Ducts from the inlets led into a single duct which had an exit at the body base. The area of the throat of the model inlets (10.4 cm^2 (1.612 $in.^2$)) in the present investigation corresponded to that for the cruise condition. The duct exit shown in figure 2 was used in the present investigation.

The two model lengths investigated were representative of a short single-place model (fig. 1(a)) and a long two-place model (fig. 1(b)). Photographs of the two-place model with an afterbody fuel tank are shown in figure 3. The single-place model was converted to a two-place model by adding a fuselage spacer block and a canopy spacer block with shims as shown in figure 4.

In addition to the modification to the fuselage length, several additional model changes were investigated. A larger vertical tail, which had an area 10 percent greater than the standard vertical tail (fig. 5) was tested. External fuel tanks, each having a capacity of 2.46 cubic meters (650 U.S. gallons) were pylon mounted on the fuselage (fig. 6(a)) and on the wings (fig. 6(b)). One configuration had an afterbody fuel tank which was designed

according to the area rule for a capacity of approximately 1.08 cubic meters (286 U.S. gallons). (See fig. 7.) The effect of leading-edge-flap deflection was also investigated. The model configurations are identified herein as follows:

Configuration	Fuselage length	Vertical tail	Center-line fuel tank	Wing tanks	Afterbody fuel tank	Leading-edge-flap deflection, δ_n, deg
1	Short	Standard	Off	Off	Off	-7.5
2	Long	Standard	Off	Off	Off	-7.5
3	Long	None	Off	Off	Off	-7.5
4	Long	Standard	On	Off	Off	-7.5
5	Long	Standard	On	On	Off	-7.5
6	Long	Large	Off	Off	Off	-7.5
7	Long	Large	Off	Off	Off	0
8	Long	Standard	Off	Off	On	-7.5

Instrumentation

A six-component strain-gage balance, which was housed in the model fuselage, was used for determining the overall forces and moments on the model. The angle of attack was varied with the tunnel-sting-support system and was corrected for flexibility under aerodynamic load of the balance, the model sting, and the sting extension.

A static-pressure orifice was located within the chamber surrounding the strain-gage balance and was connected to a pressure transducer. A static-pressure tube with three orifices was attached to the rim of the body base and connected to a pressure transducer. Two other static-pressure orifices were located on the sides of the sting adjacent to the base of the body and were joined to a common tube and connected to a pressure transducer. (These static pressures were used in the base-pressure corrections.) A sting-mounted rake was used at the duct exit when mass flow and internal-drag measurements were made. The rake consisted of 2 static-pressure tubes and 12 total-pressure tubes, and a manometer was used to measure the pressures.

TEST CONDITIONS

All the tests were made with fixed transition on the model as recommended in reference 7. Strips of No. 120 carborundum grains 0.275 centimeter (0.1 in.) wide were shellacked on the upper and lower surfaces of the wing and horizontal tail at 10 percent

chord, on both sides of the vertical tail at 10 percent chord, on the fuselage 1.27 cm (0.5 in.) behind the nose apex and on the upper and lower inlet surfaces 0.64 cm (0.25 in.) behind the leading edge. The 2.46-cubic-meter (650 U.S. gallon) capacity external fuel tanks were tested without fixed transition. Pitch tests were made at an angle of sideslip of 0° with the wings of the model in the horizontal plane of the tunnel. The pitch tests were made at Mach numbers from 0.6 to 1.2 at a stagnation pressure of 3/4 atmosphere through an angle-of-attack range from approximately -2° to 24°. Configuration 1 was also investigated through a large angle-of-attack range (-11° to 30°) at a Mach number of 0.80 to determine the pitch-up characteristics of the model, for this test a stagnation pressure of 3/4 atmosphere was used at angles of attack from -11° to 22° and of 1/2 atmosphere at angles of attack from 22° to 30°. All remaining tests were sideslip tests at fixed nominal values of angle of attack (obtained by the use of bent couplings with angles between the model sting and the tunnel sting of 0°, 5°, 10°, and 15°). The sideslip tests were made with the model wings in the vertical plane of the tunnel at Mach numbers from 0.60 to 1.20 at a stagnation pressure of 1/2 atmosphere through an angle-of-sideslip range from approximately -4° to 15°.

The variation of Reynolds number (based on the mean aerodynamic chord $\bar{c}$) with Mach number for stagnation pressures of 1/2 and 3/4 atmosphere is shown in figure 8. The stagnation temperature was approximately 322° K (120° F) at all Mach numbers during the investigation.

All the configurations were investigated with internal flow in the model. The static pressure in the chamber surrounding the strain-gage balance, at the side of the sting at the fuselage base, and at the rim of the fuselage base were recorded at each test data point. One internal mass flow and internal drag test was made to determine these quantities at several angles of attack at each Mach number through the Mach number range.

CORRECTIONS

The external-drag coefficients C_D and C_D' were corrected by adjusting the values of static pressure in the balance chamber and at the rim of the fuselage base to the free-stream value. The external-drag coefficients also include the correction for the internal-drag coefficient $C_{D,i}$ (fig. 9) determined from the internal mass flow and internal drag test of configuration 1.

The lift and pitching-moment coefficients were not corrected for internal flow. A previous investigation indicated the maximum correction to lift coefficient occurred at the highest angle of attack and amounted to only 0.005.

At subsonic Mach numbers, the interference effect of the tunnel boundary on the flow over a model in the test region near the center line of the tunnel has been made

negligible by means of a slotted test section. Data are presented herein at transonic Mach numbers of 1.03 and 1.20. The effect of tunnel-boundary interference (tunnel-boundary-reflected compression and expansion disturbances) on the data at a Mach number of 1.03 was probably small and is believed to have been confined primarily to affecting the drag data. The data at a Mach number of 1.20 are considered free of tunnel-boundary interference. No corrections have been made to the data at a Mach number of 1.03 for tunnel-boundary interference except for the partial correction for tunnel-boundary interference inherent in the base-pressure correction.

No sting-interference corrections have been made to the data except for the partial correction for sting interference inherent in the base-pressure correction.

Accuracy

The accuracy of the data, based primarily on the static calibrations and the repeatability of the data, is estimated to be as follows:

C_L	±0.01
C_D	±0.0012
C_D'	±0.0018
C_m	±0.003
C_n	±0.0004
C_l	±0.0003
C_Y	±0.002
α, deg	±0.1
β, deg	±0.1
M	±0.003

PRESENTATION OF RESULTS

The basic longitudinal aerodynamic characteristics are presented in figures 10 to 13, and the basic aerodynamic characteristics in sideslip are presented in figures 14 to 17. These basic results for specific model configurations are presented in the figures indicated in the following list:

Summary data on performance and longitudinal-stability derivatives are shown in figures 18 to 20. The derivatives C_{L_α} and $C_{m_{C_L}}$ in the figures are for a lift coefficient of approximately zero. Summary data on lateral-stability derivatives are shown in figures 21 to 24. The derivatives C_{n_β}, C_{l_β}, and C_{Y_β} (figs. 21 to 24) are for an angle of sideslip of approximately 0°. The figures containing these summary results for specific models are indicated, as follows:

Approximate values of angle of attack are given on the basic and summary sideslip figures. More accurate values of angle of attack for the sideslip data at the various test Mach numbers and stagnation pressures are given in the following table:

M	Stagnation pressure, atm	α, deg			
1.20	1/2	0.0	5.4	10.7	16.0
1.03	1/2	.0	5.4	10.7	16.0
.95	1/2	.0	5.4	10.7	15.9
.90	1/2	.0	5.4	10.7	15.8
.80	1/2	.0	5.3	10.6	15.7
.60	1/2	.0	5.2	10.4	15.5

DISCUSSION

Longitudinal Aerodynamic Characteristics

An increase in fuselage length (figs. 10 and 18) had negligible effect on the longitudinal aerodynamic characteristics of the model. The fuselage-mounted center-line external fuel tank (configuration 4, figs. 11 and 19) had little effect on the longitudinal stability of the model, but caused a reduction in maximum lift-drag ratio of from 3.6 to 10.7 percent through the Mach number range. The wing tanks in combination with the fuselage tank reduced the maximum lift-drag ratio about 20 percent and caused a shift in trim to higher lift coefficients at all Mach numbers. The afterbody fuel tank (configuration 8, figs. 12 and 20) had negligible effect on the longitudinal aerodynamic characteristics.

Model configuration 1 (the short fuselage model) was investigated through an angle-of-attack range of -12° to 30° at a Mach number of 0.80 (fig. 13). These results (fig. 13(b)) indicate that a pitch-up occurred for this configuration in the angle-of-attack range from 21° to 27°.

Lateral Stability

The directional-stability derivative C_{n_β} of model configurations 1 and 2 was positive (that is, directionally stable) at $\alpha \approx 5.3^{\circ}$ at all test values of Mach number and angle of sideslip (fig. 14(a)), and also at $\alpha \approx 15.8^{\circ}$ except at the highest values of angle of sideslip (fig. 14(b)). An increase in body length reduced the directional stability at all test Mach numbers by a small amount at $\alpha \approx 5.3^{\circ}$ and by a generally larger amount at $\alpha \approx 15.8^{\circ}$ (figs. 14(a), 14(b), and 21).

The derivative C_{l_β} of model configurations 1 and 2 was negative (positive dihedral effect) at $\alpha \approx 5.3^{\circ}$ and $\alpha \approx 15.8$ for all values of angle of sideslip and Mach numbers

investigated (figs. 14(a) and (b)). However, there was an appreciable decrease in the magnitude of C_{l_β} with change in angle of attack from 5.3° to 15.8° at Mach numbers of 0.60 and 0.80.

Figure 22 shows that the large vertical tail (10-percent increase in area) increased the directional stability of model configuration 2 by approximately 12 percent at $\alpha \approx 5.3^\circ$ and 35 percent at $\alpha \approx 15.8^\circ$ throughout the Mach number range. (See also figs. 15(b) and 15(d).) This improvement in directional stability was caused by the increase in area of the vertical tail and was sufficient to overcome the loss in directional stability caused by the increase in fuselage and canopy length.

The external fuel-tank configuration 4 (which includes fuselage center-line tank) and configuration 5 (which includes fuselage center-line tank and wing tanks) were directionally stable at $\alpha \approx 5.3^\circ$ at all test Mach numbers and angles of sideslip (fig. 16(a)). Model configuration 5 was also directionally stable at $\alpha \approx 15.8$ at all test Mach numbers and angles of sideslip (fig. 16(b)). Model configuration 4, however, had either neutral directional stability or was directionally unstable over the angle-of-sideslip range at $\alpha \approx 15.8^\circ$ at Mach numbers of 0.90, 0.95, and 1.20. At the other test Mach numbers, configuration 4 at $\alpha \approx 15.8^\circ$ was also directionally unstable at certain values of sideslip angle. The addition of the fuselage-mounted fuel tank reduced C_{n_β} substantially, by an increment which was roughly the same at $\alpha \approx 5.3^\circ$ and $\alpha \approx 15.8^\circ$ at all test Mach numbers (figs. 16(a), 16(b), and 23). The addition of the wing tanks had small effect on C_{n_β} at subsonic test Mach numbers at $\alpha \approx 5.3^\circ$ but increased C_{n_β} at supersonic test Mach numbers at $\alpha \approx 5.3^\circ$ and at all test Mach numbers at $\alpha \approx 15.8^\circ$.

The lateral-stability derivative C_{l_β} for configurations 4 and 5 was negative (positive dihedral effect) at all test conditions except at a Mach number of 0.60 and $\alpha \approx 15.8^\circ$ where the derivative was positive in a small range of angles of sideslip up to about 4° for configuration 4 (figs. 16(a), 16(b), and 23).

The leading-edge-flap deflection, figures 17 and 24, had no significant effect on the lateral stability derivatives C_{n_β} and C_{l_β} for any test condition used in the investigation.

CONCLUDING REMARKS

An investigation was made at Mach numbers from 0.60 to 1.20 of the static longitudinal and lateral stability characteristics of various configurations of a 1/22-scale model of a supersonic fighter-bomber airplane. Configurations included a single-place short-fuselage model and a two-place long-fuselage model. The two-place model was

investigated with external stores, afterbody fuel tank, larger vertical tail, and wing-leading-edge-flap deflections of 0° and -7.5°.

The effect of configuration modifications on longitudinal stability and trim was small. The external stores caused a shift in trim to higher lift coefficients and a substantial increase in drag.

A decrease in directional stability caused by lengthening the fuselage can be regained by a 10-percent increase in the area of the vertical tail. The fuselage-mounted center-line fuel tank decreased the directional stability at all test conditions. With this configuration, the model was directionally stable at low angles of attack but unstable at an angle of attack of 15.8° at Mach numbers of 0.90, 0.95, and 1.20. The model with the fuselage-mounted center-line fuel tank, in combination with the wing tanks, was generally directionally stable at all test conditions. Deflection of the leading-edge flap had no signnigicant effect on the lateral stability of the model.

Langley Research Center,
National Aeronautics and Space Administration,
Langley Station, Hampton, Va., June 23, 1966.

REFERENCES

1. Appich, W. H., Jr.; Oehman, Waldo I.; and Gregory, Donald T.: Aerodynamic Characteristics of Three Versions of a Supersonic Airplane Model With a 45° Sweptback Midwing at Mach Numbers of 1.57 and 2.01. NASA MEMO 12-6-58L, 1959.

2. Luoma, Arvo A.: Transonic Wind-Tunnel Investigation of the Static Longitudinal Stability and Performance Characteristics of a Supersonic Fighter-Bomber Airplane. NASA TM X-513, 1961.

3. Luoma, Arvo A.: Transonic Wind-Tunnel Investigation of the Static Stability and Control Characteristics of a Supersonic Fighter-Bomber Airplane. NASA TM X-591, 1961.

4. Foster, Gerald V.; and Kyle, Robert G.: Aerodynamic Characteristics of a 1/22-Scale Model of a Fighter Airplane With an Extended Forebody and Other Modifications at Mach Numbers of 1.57 and 2.01. NASA TM X-833, 1963.

5. Ferris, James C.: Effects of External Stores on Performance and Stability of a Supersonic Fighter-Bomber Airplane. NASA TM X-1218, 1966.

6. Mechtly, E. A.: The International System of Units – Physical Constants and Conversion Factors. NASA SP-7012, 1964.

7. Braslow, Albert L.; and Knox, Eugene C.: Simplified Method for Determination of Critical Height of Distributed Roughness Particles for Boundary-Layer Transition at Mach Numbers From 0 to 5. NACA TN 4363, 1958.

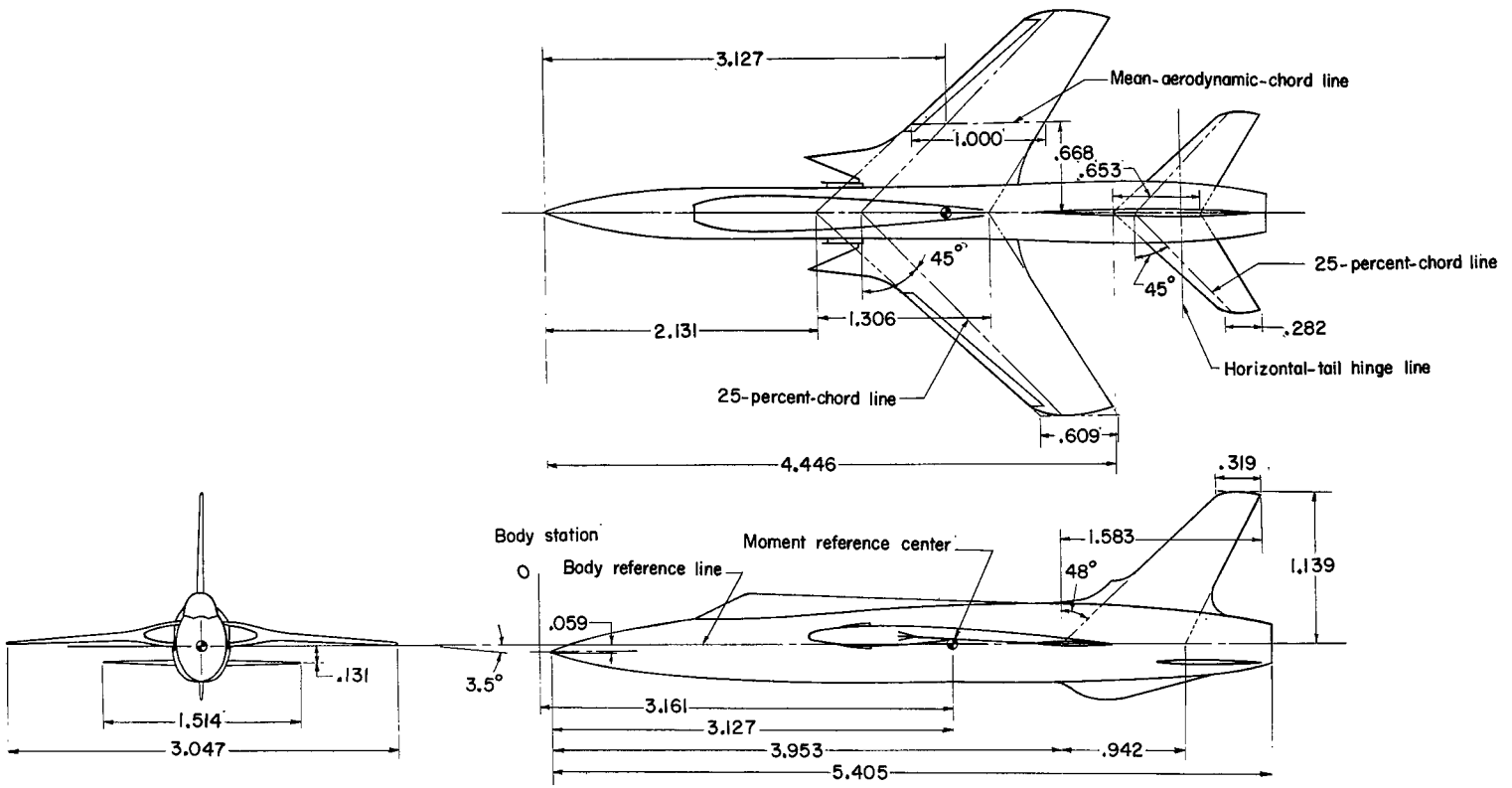

(a) Short single-place model.

Figure 1.- General arrangement of supersonic fighter-bomber airplane. All dimensions are in terms of the mean aerodynamic chord $\bar{c}$. $\bar{c}$ = 15.91 cm (6.264 in.).

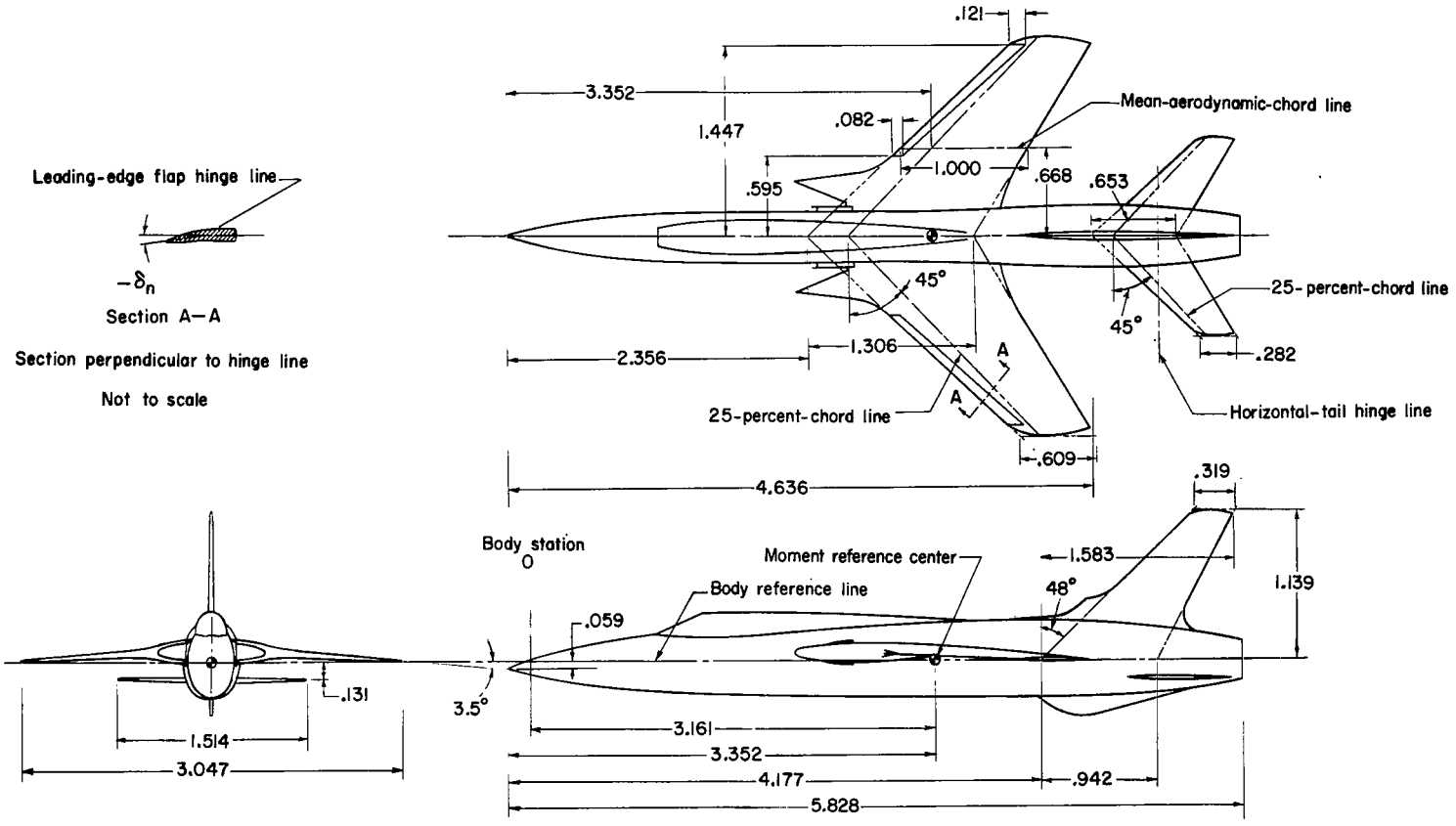

(b) Long two-place model.

Figure 1.- Concluded.

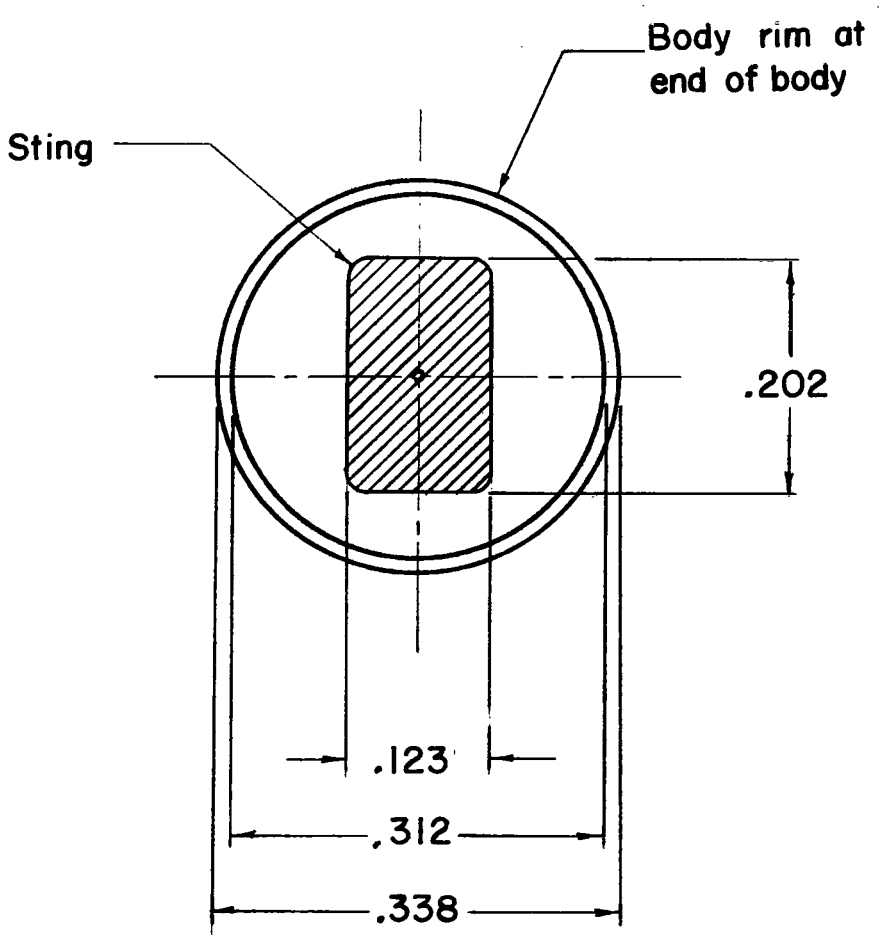

Figure 2.- Duct exit used with supersonic inlet (cruise condition) and sting cross section at end of body. Duct exit area = 13.06 cm^2 (2.024 sq in.). All dimensions are in terms of the mean aerodynamic chord $\bar{c}$. $\bar{c}$ = 15.91 cm (6.264 in.).

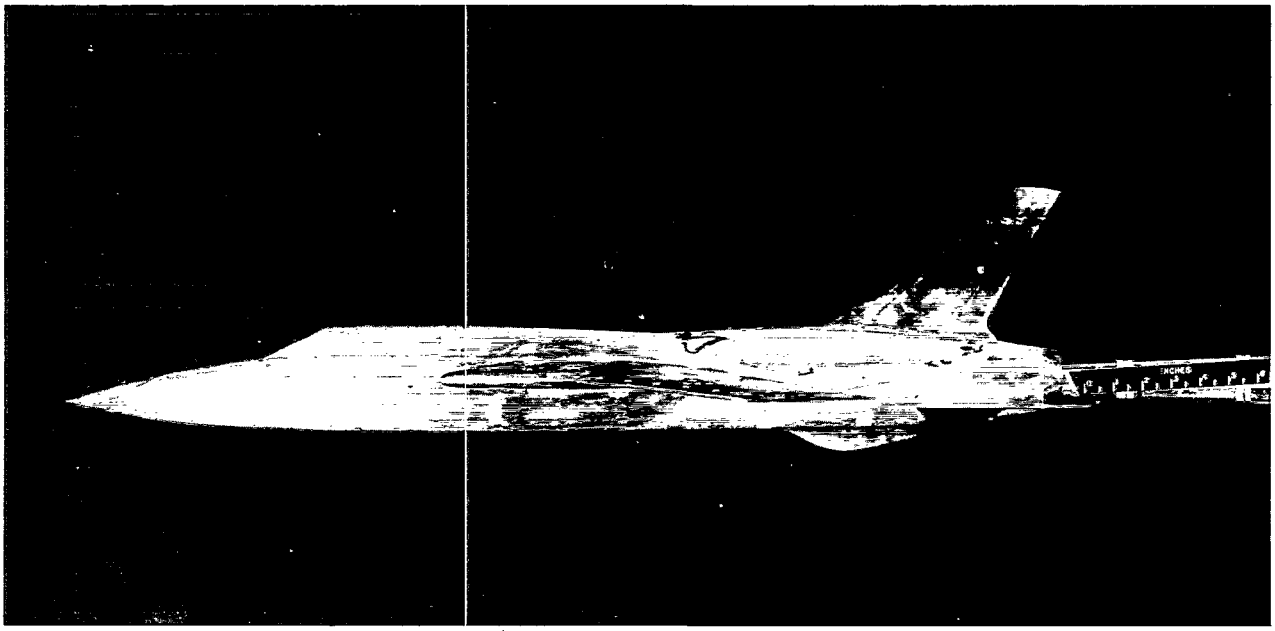

(a) Side view. L-62-6080

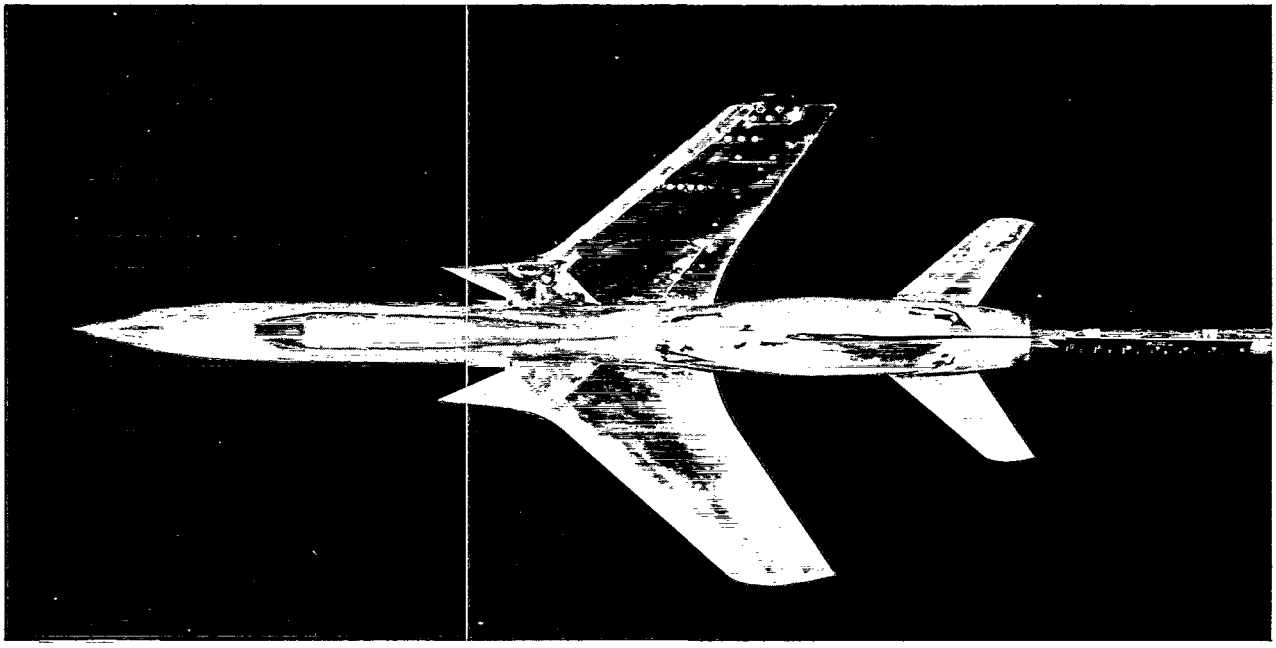

(b) Planform view. L-62-6078

Figure 3.- Model configuration 8.

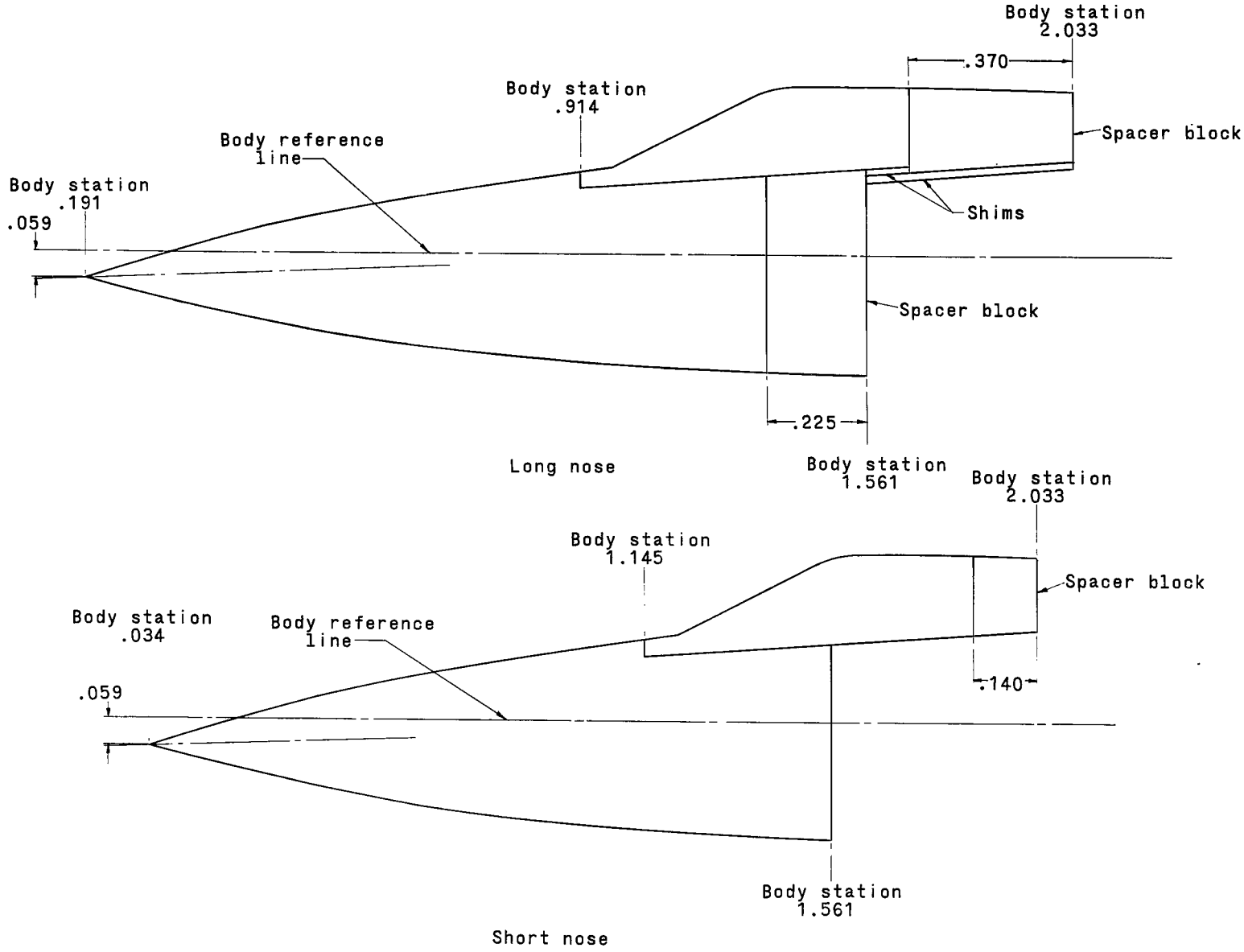

Figure 4.- Model modifications. All dimensions are in terms of the mean aerodynamic chord $\bar{c}$. $\bar{c}$ = 15.91 cm (6.264 in.).

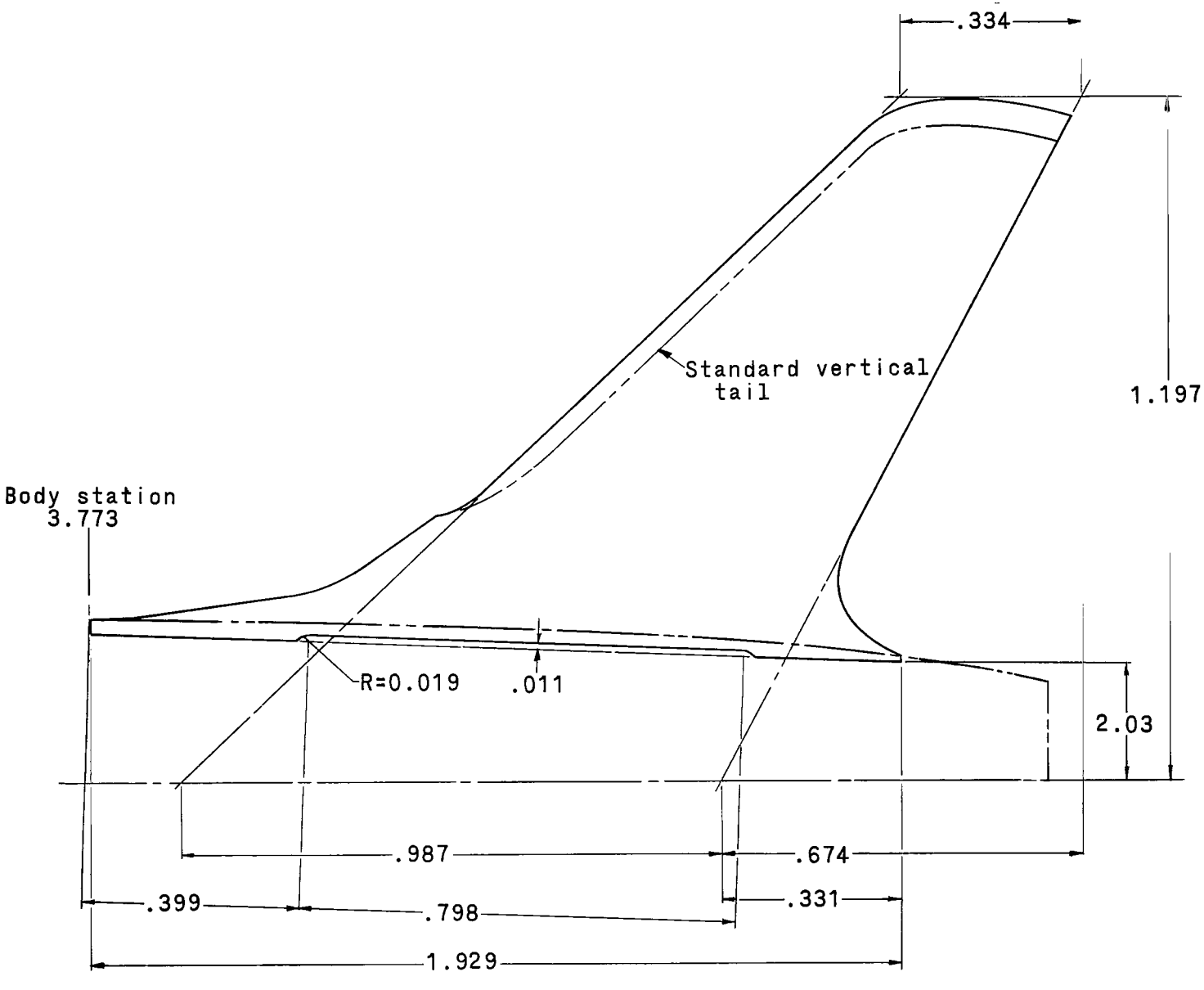

Figure 5.- Vertical tail with 110 percent area of standard vertical tail. All dimensions are in terms of the mean aerodynamic chord $\bar{c}$. $\bar{c}$ = 15.91 cm (6.264 in.).

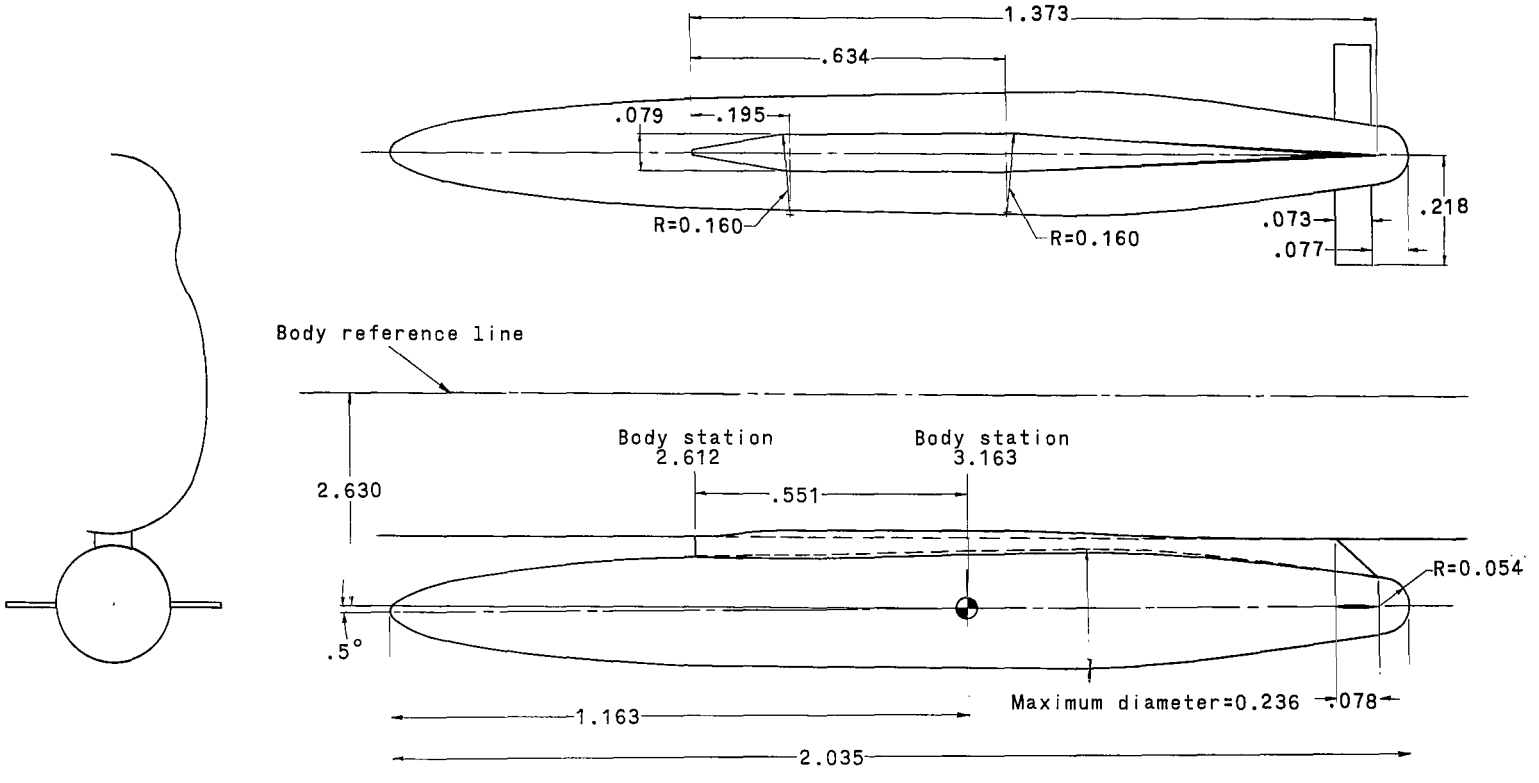

(a) Center-line fuselage-mounted tank.

Figure 6.- External fuel tanks. All dimensions are in terms of the mean aerodynamic chord $\bar{c}$. $\bar{c}$ = 15.91 cm (6.264 in.).

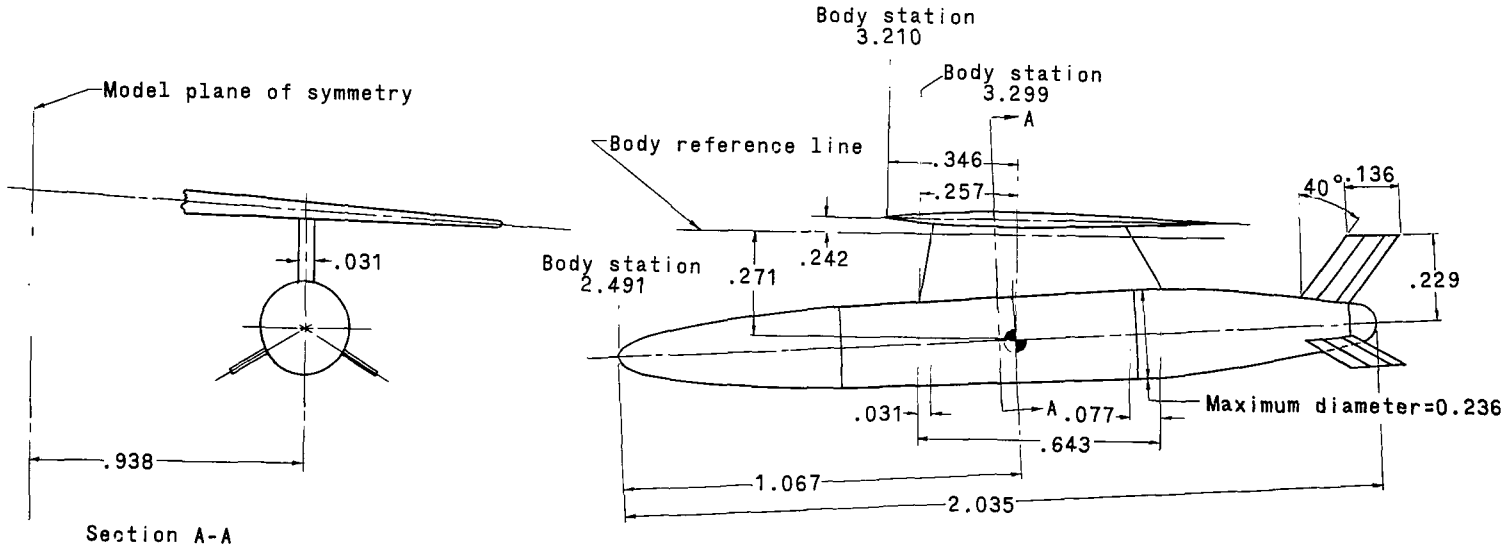

(b) Wing pylon-mounted fuel tank.

Figure 6.- Concluded.

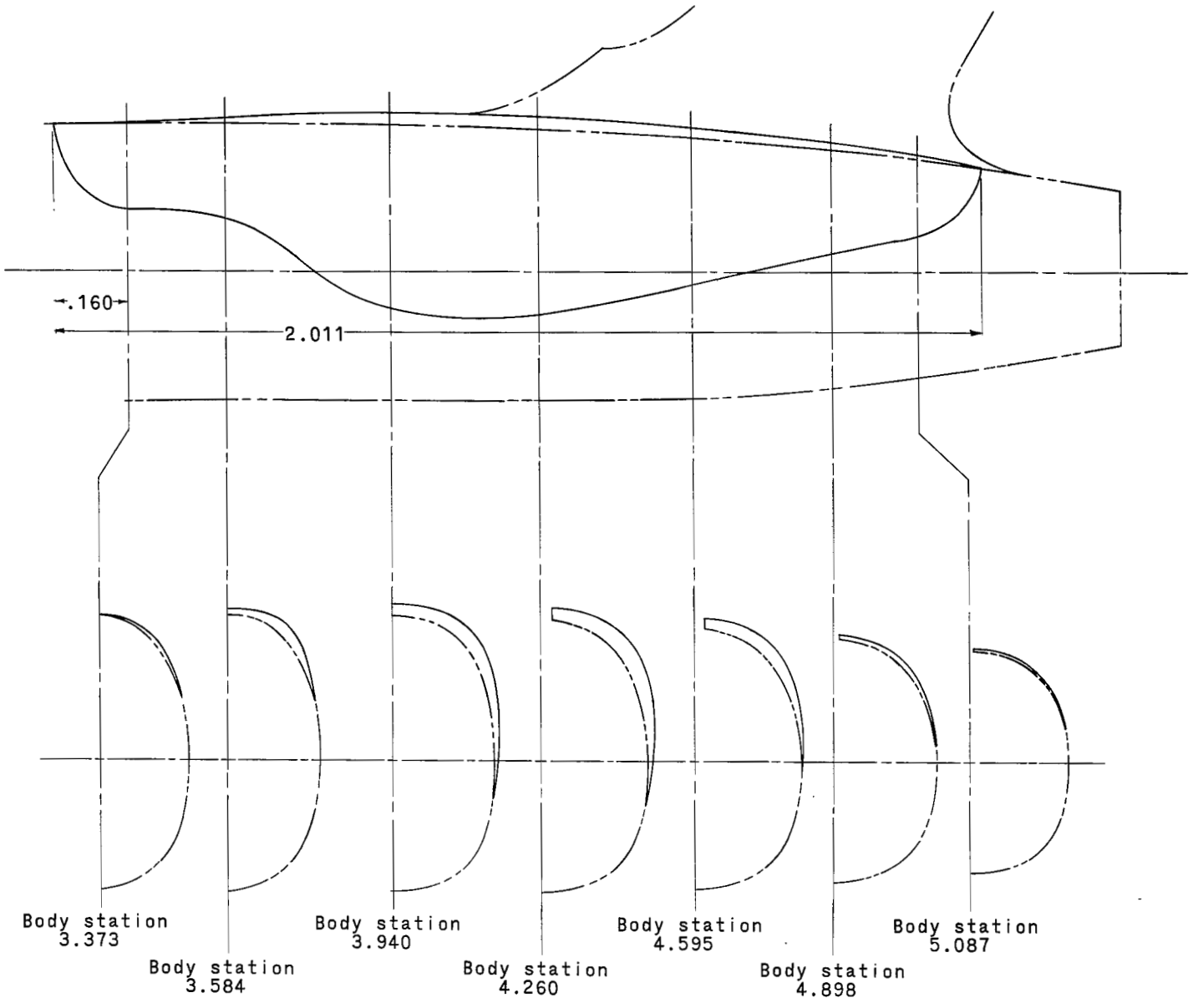

Figure 7.- Afterbody area-rule fuel tank. All dimensions are in terms of the mean aerodynamic chord $\bar{c}$. $\bar{c}$ = 15.91 cm (6.264 in.).

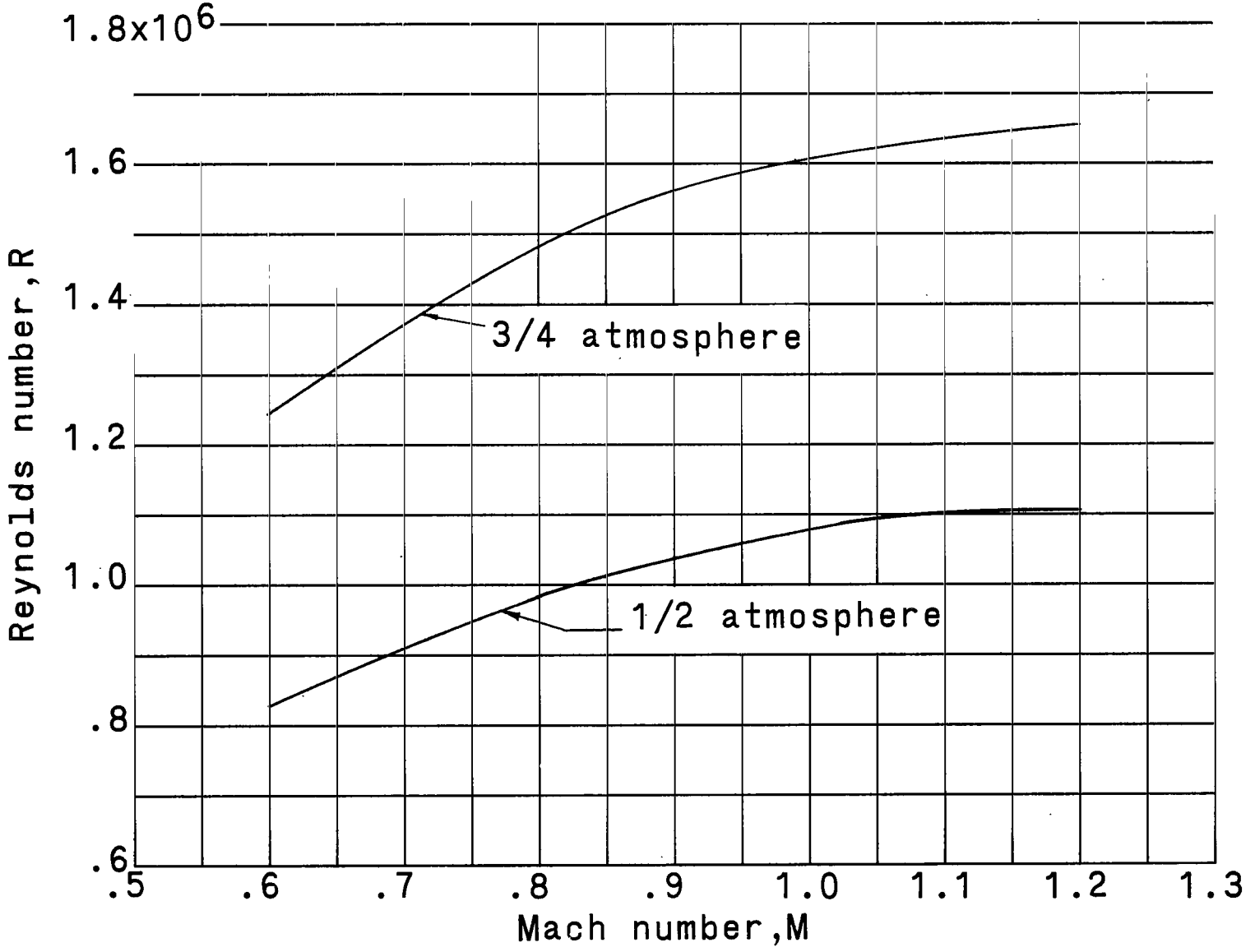

Figure 8.- Variation of average Reynolds number based on mean aerodynamic chord of 15.91 cm (6.264 in.) with Mach number in Langley 8-foot transonic pressure tunnel investigation.

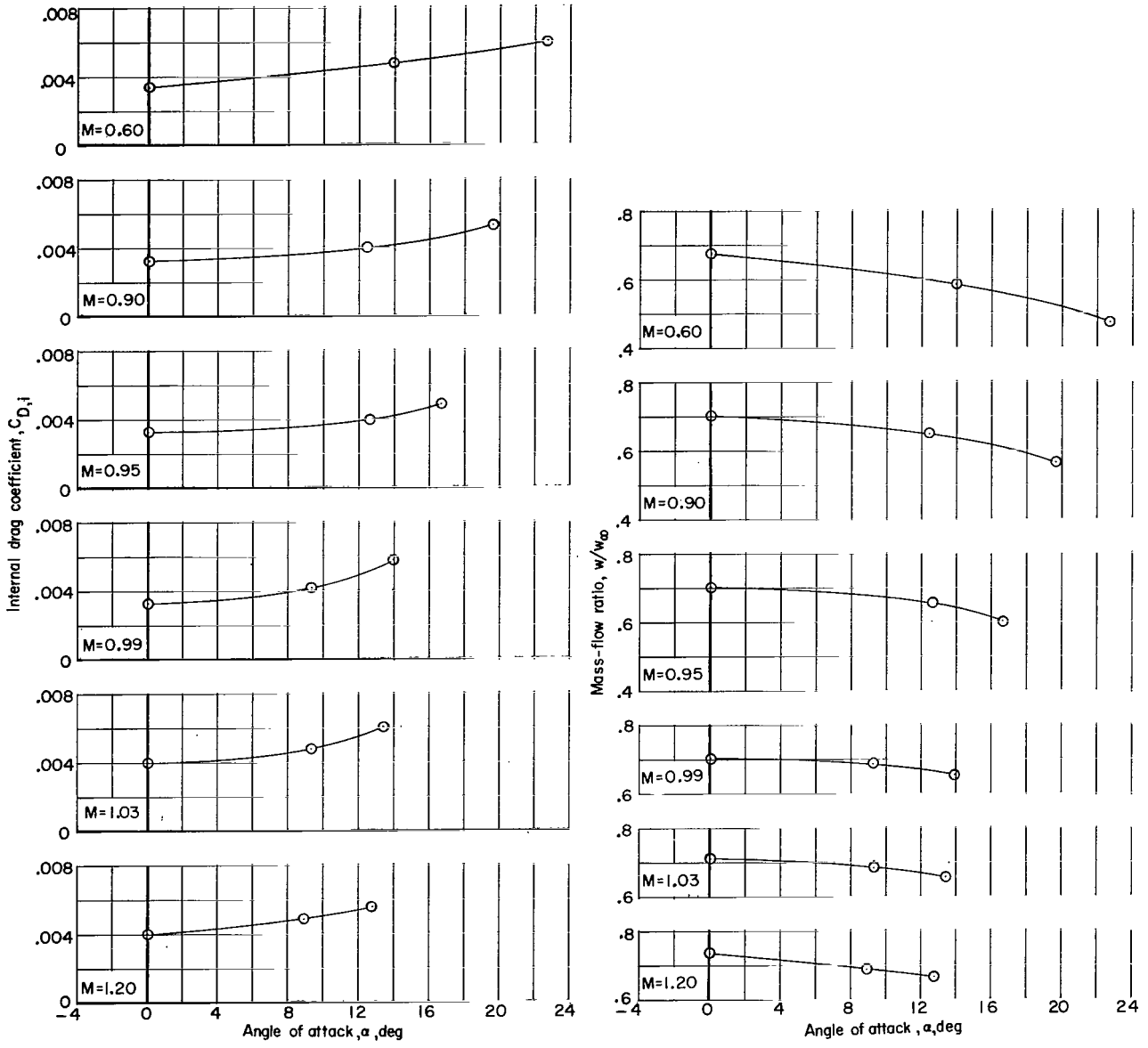

Figure 9.- Internal-drag coefficient and mass-flow ratio of model configuration 1. $\delta_h = -3^0$.

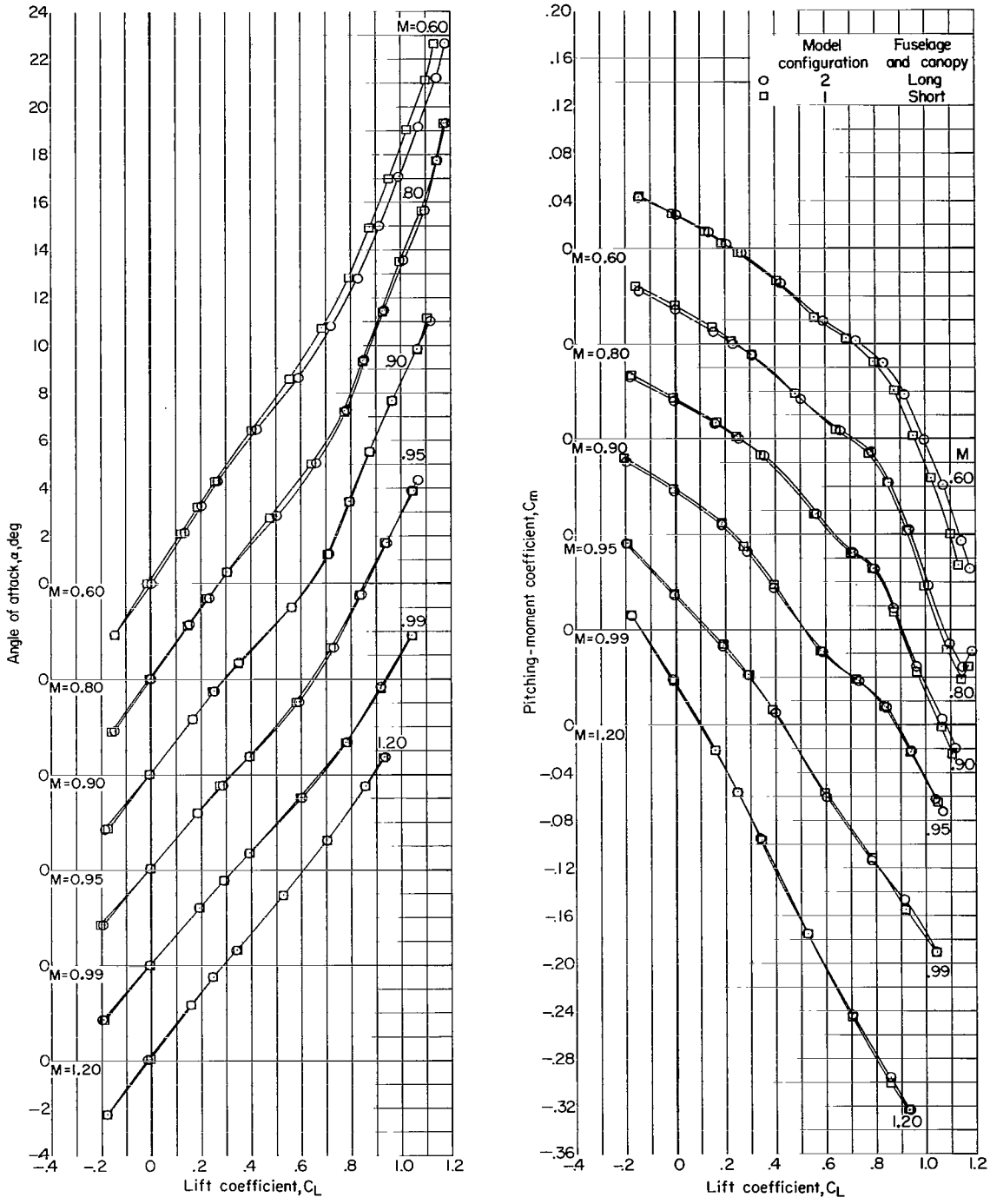

(a) Angle of attack and pitching-moment coefficient.

Figure 10.- Longitudinal aerodynamic characteristics of model configurations 1 and 2. $\delta_h = -3^0$.

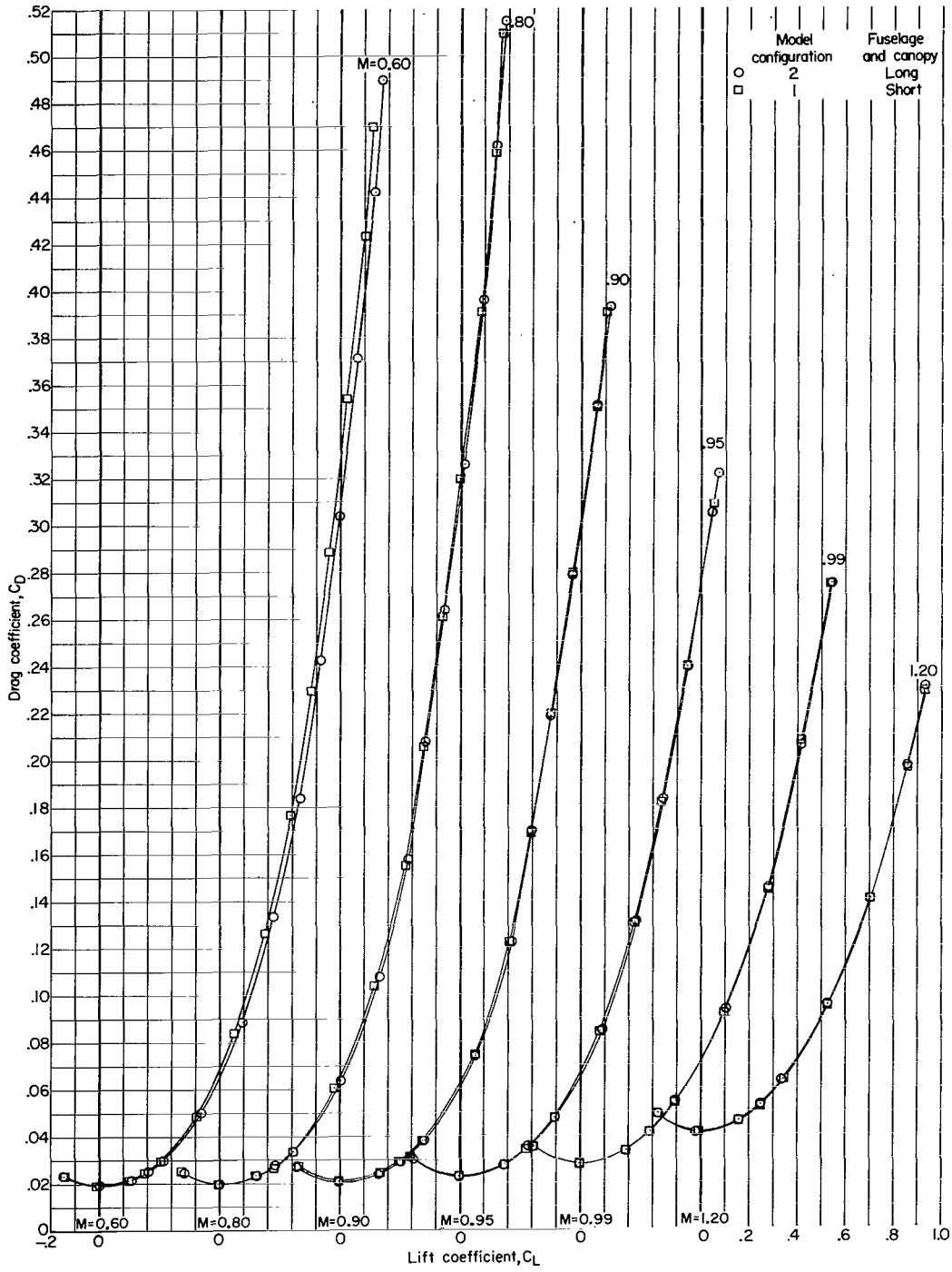

(b) Drag coefficient.

Figure 10.- Continued.

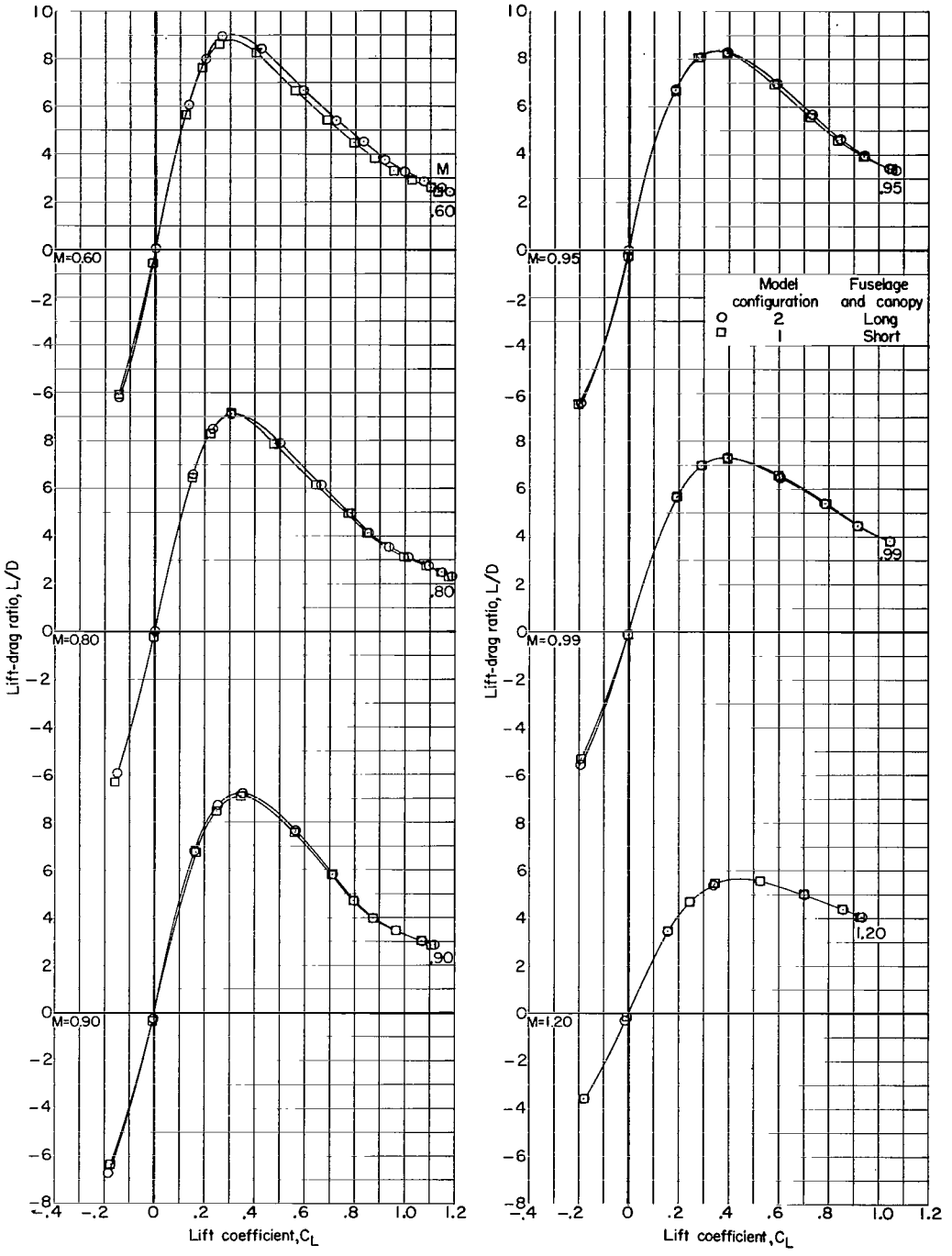

(c) Lift-drag ratio.

Figure 10.- Concluded.

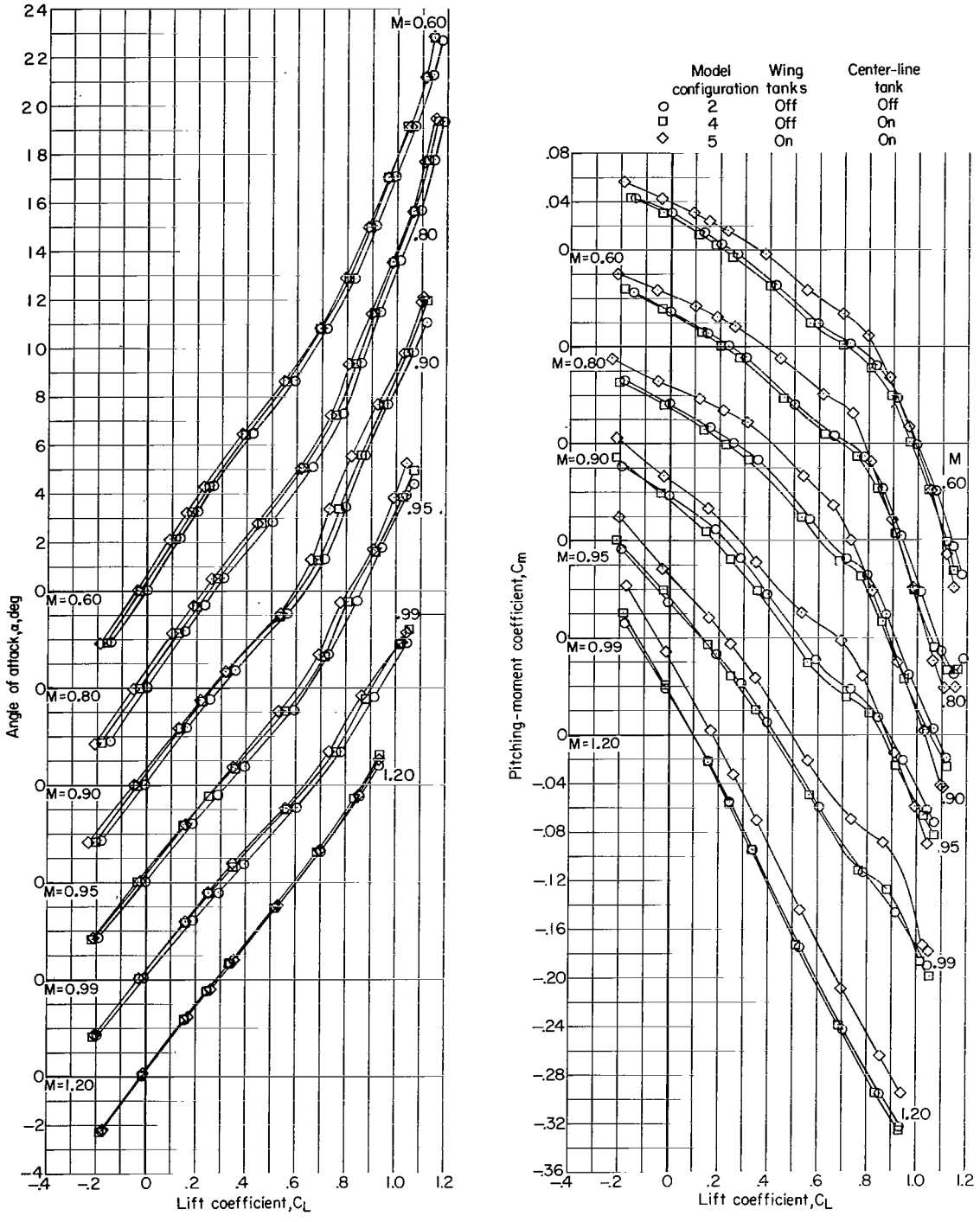

(a) Angle of attack and pitching-moment coefficient.

Figure 11.- Effect of center-line tank and wing inboard tanks on longitudinal aerodynamic characteristics. $\delta_h = -3^0$.

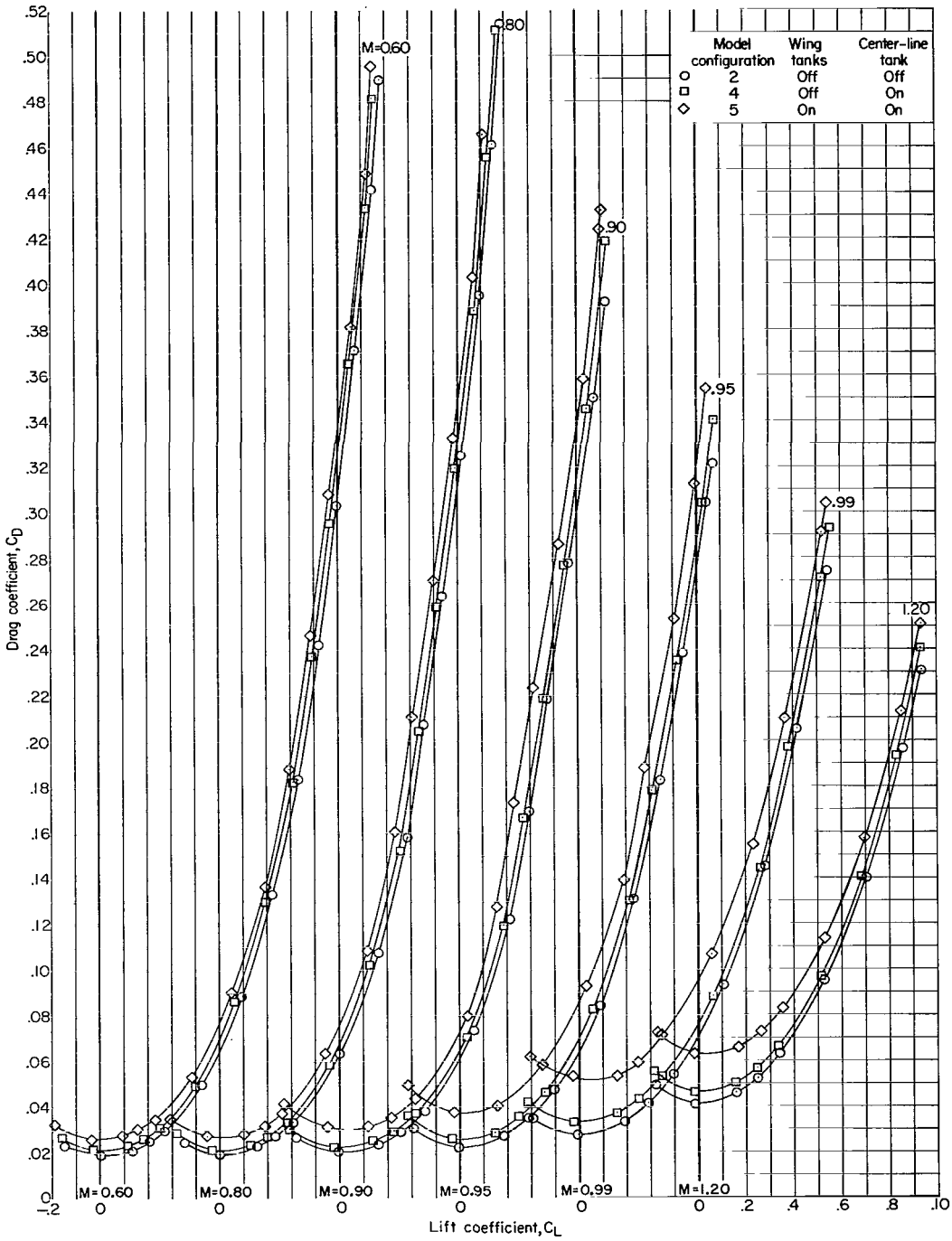

(b) Drag coefficient.

Figure 11.- Continued.

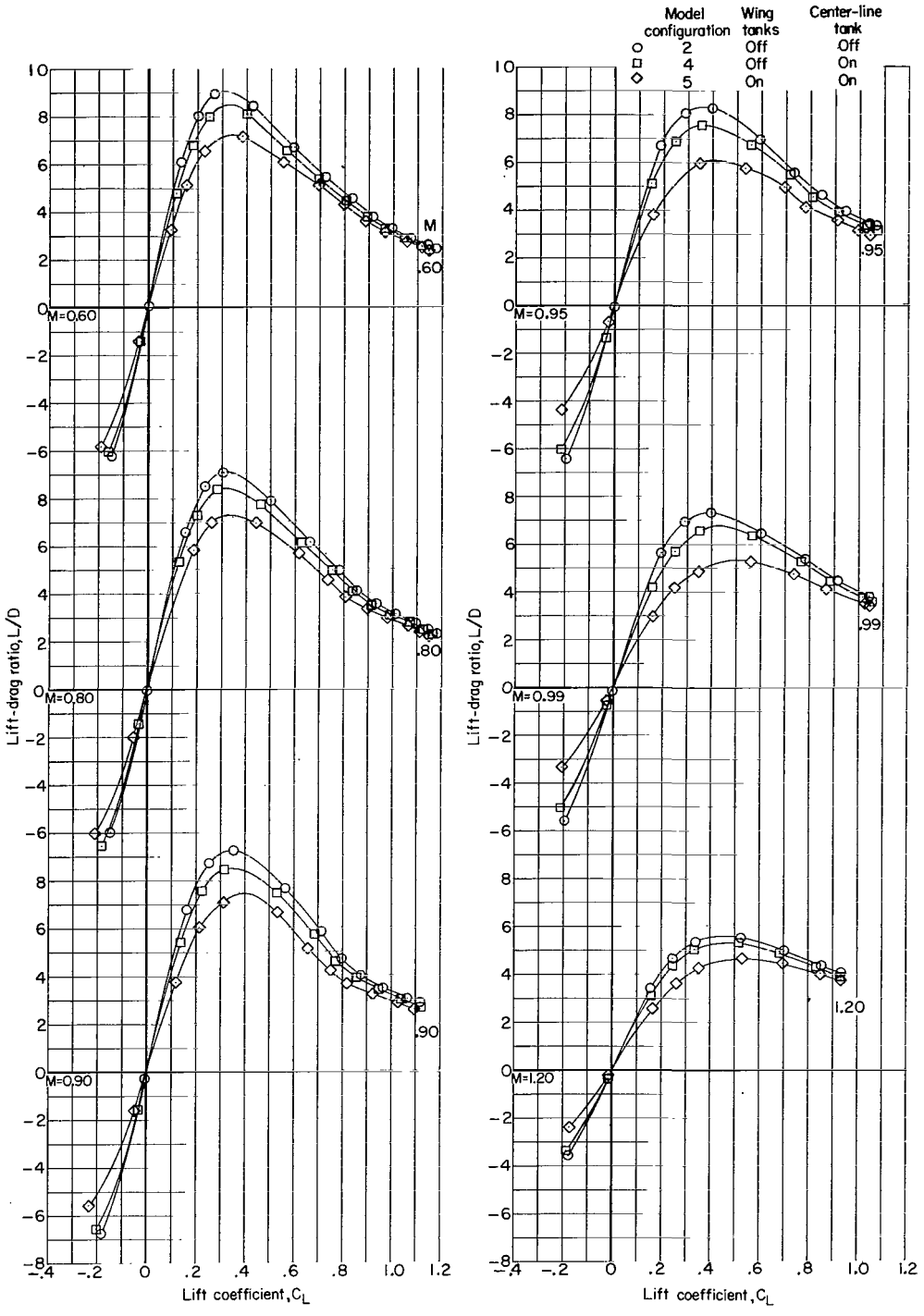

(c) Lift-drag ratio.

Figure 11.- Concluded.

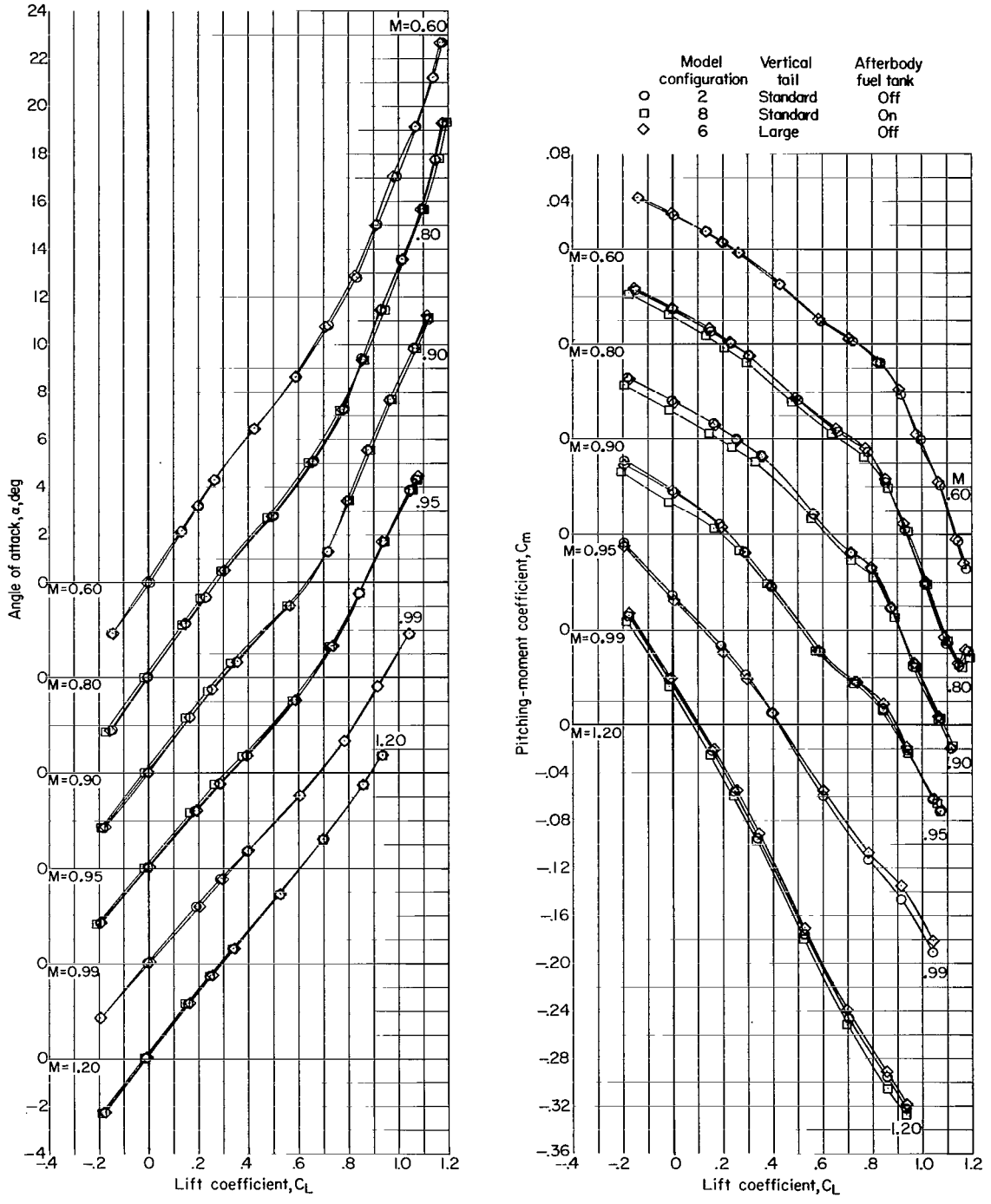

(a) Angle of attack and pitching-moment coefficient.

Figure 12.- Effect of vertical tail and afterbody fuel tank on longitudinal aerodynamic characteristics. $\delta_h = -3^0$.

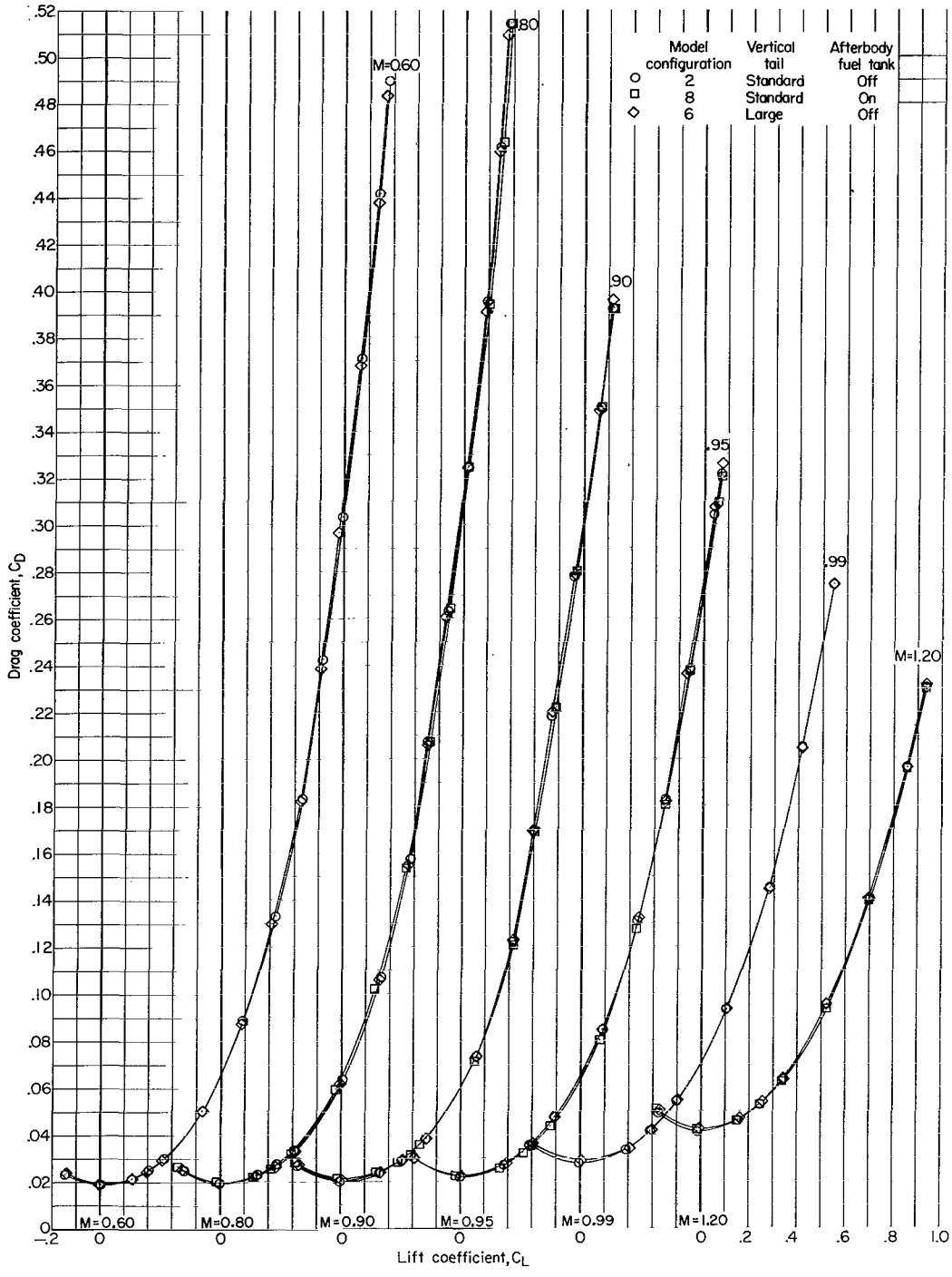

(b) Drag coefficient.

Figure 12.- Continued.

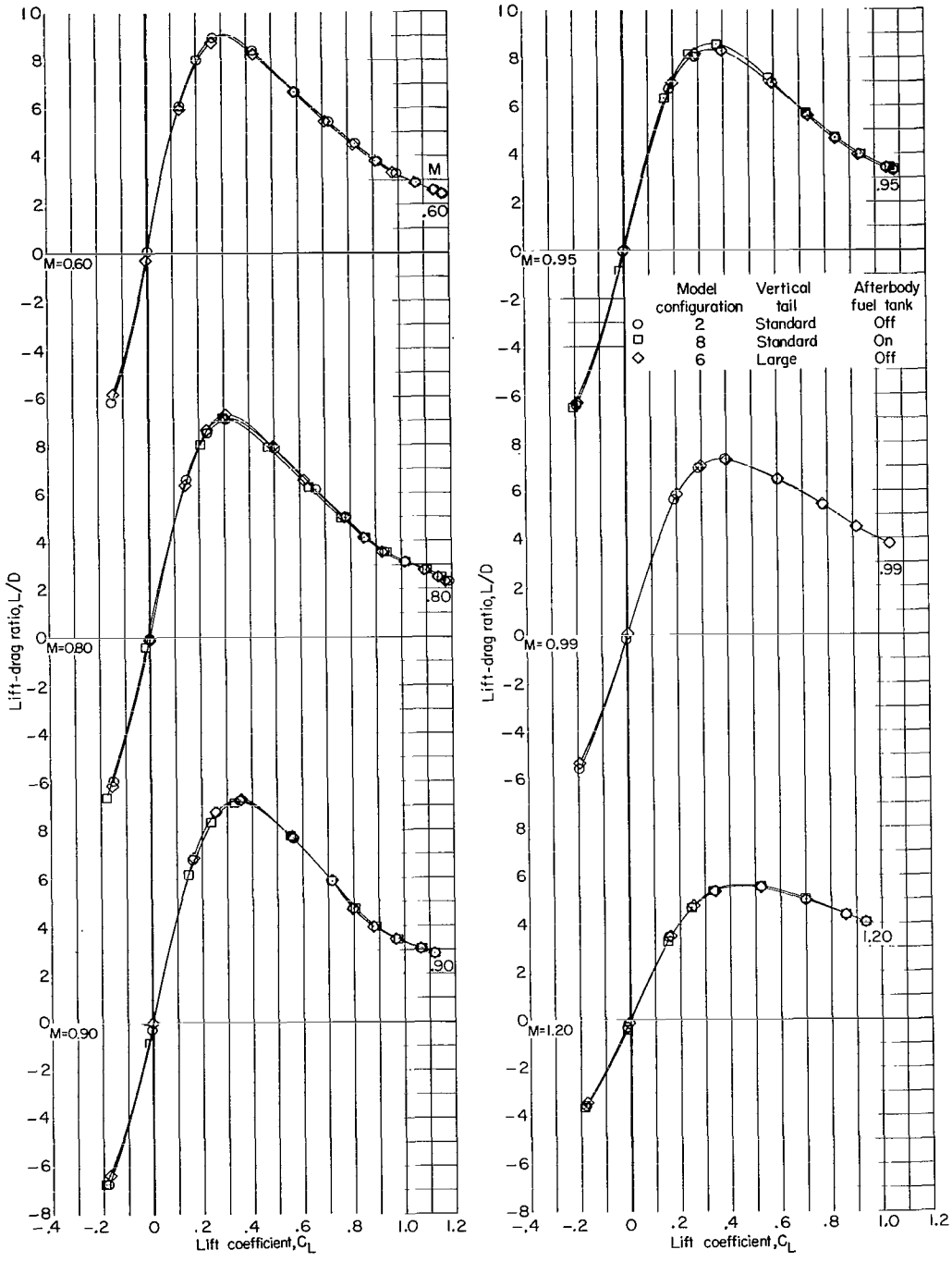

(c) Lift-drag ratio.

Figure 12.- Concluded.

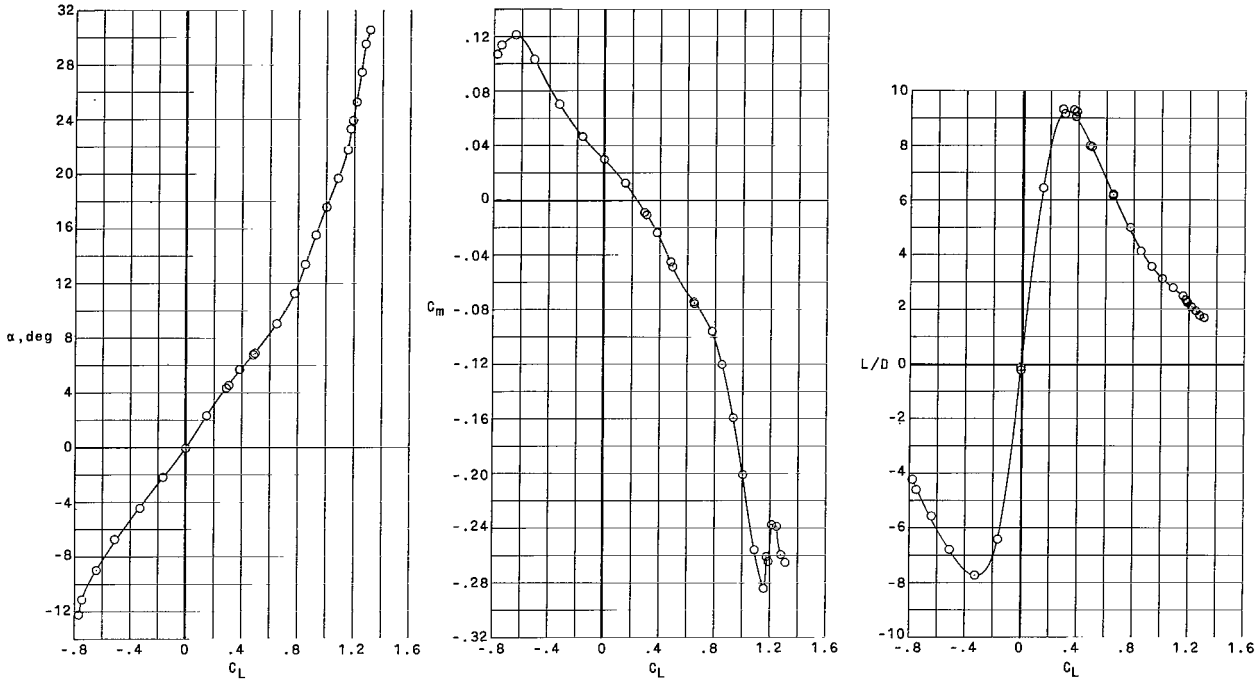

(a) Angle of attack, pitching-moment coefficient, and lift-drag ratio.

Figure 13.- Longitudinal aerodynamic characteristics of model configuration 1 (short fuselage) at large angles of attack. $\delta_h = -3^0$; M = 0.80.

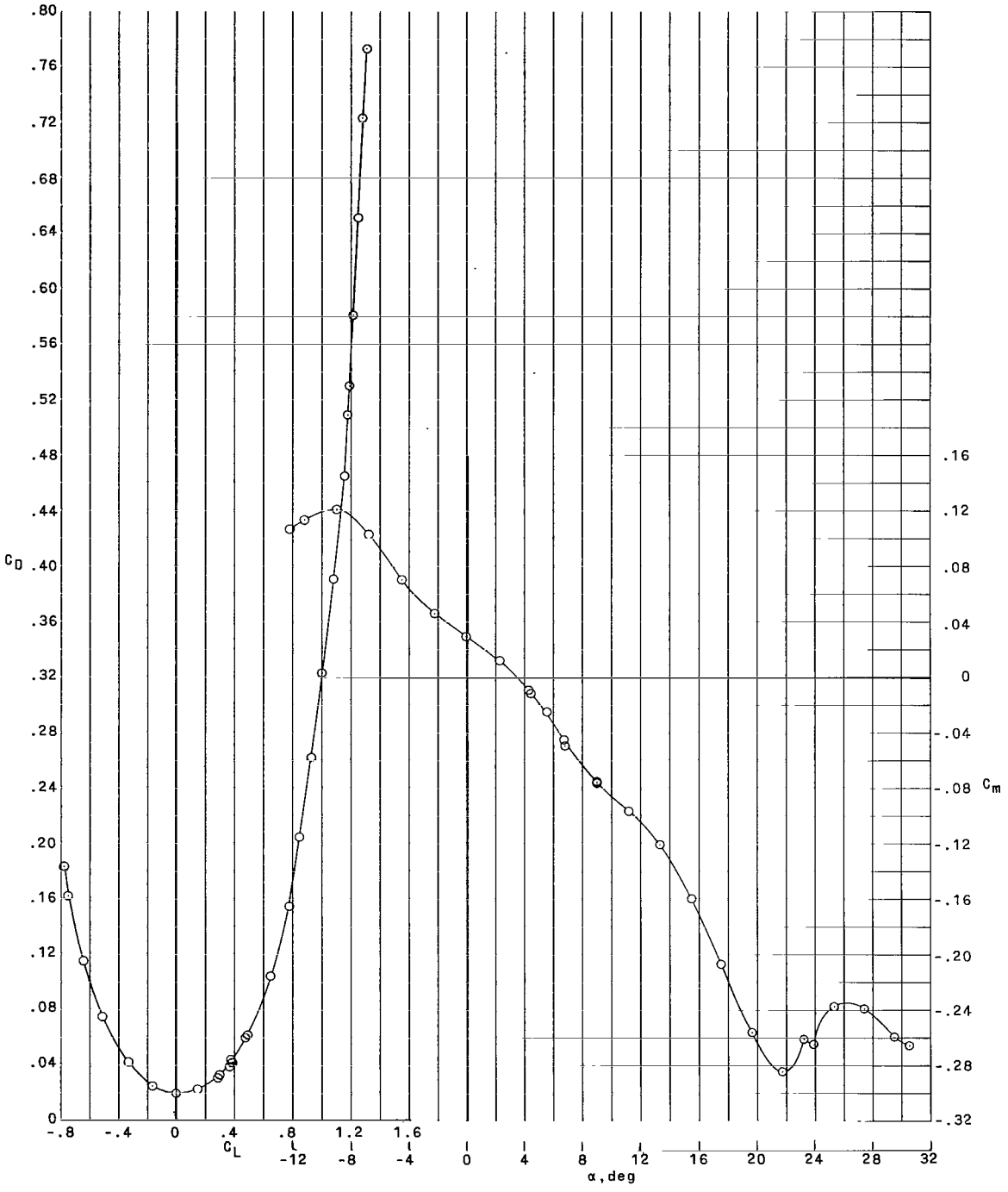

(b) Drag coefficient and pitching-moment coefficient.

Figure 13.- Concluded.

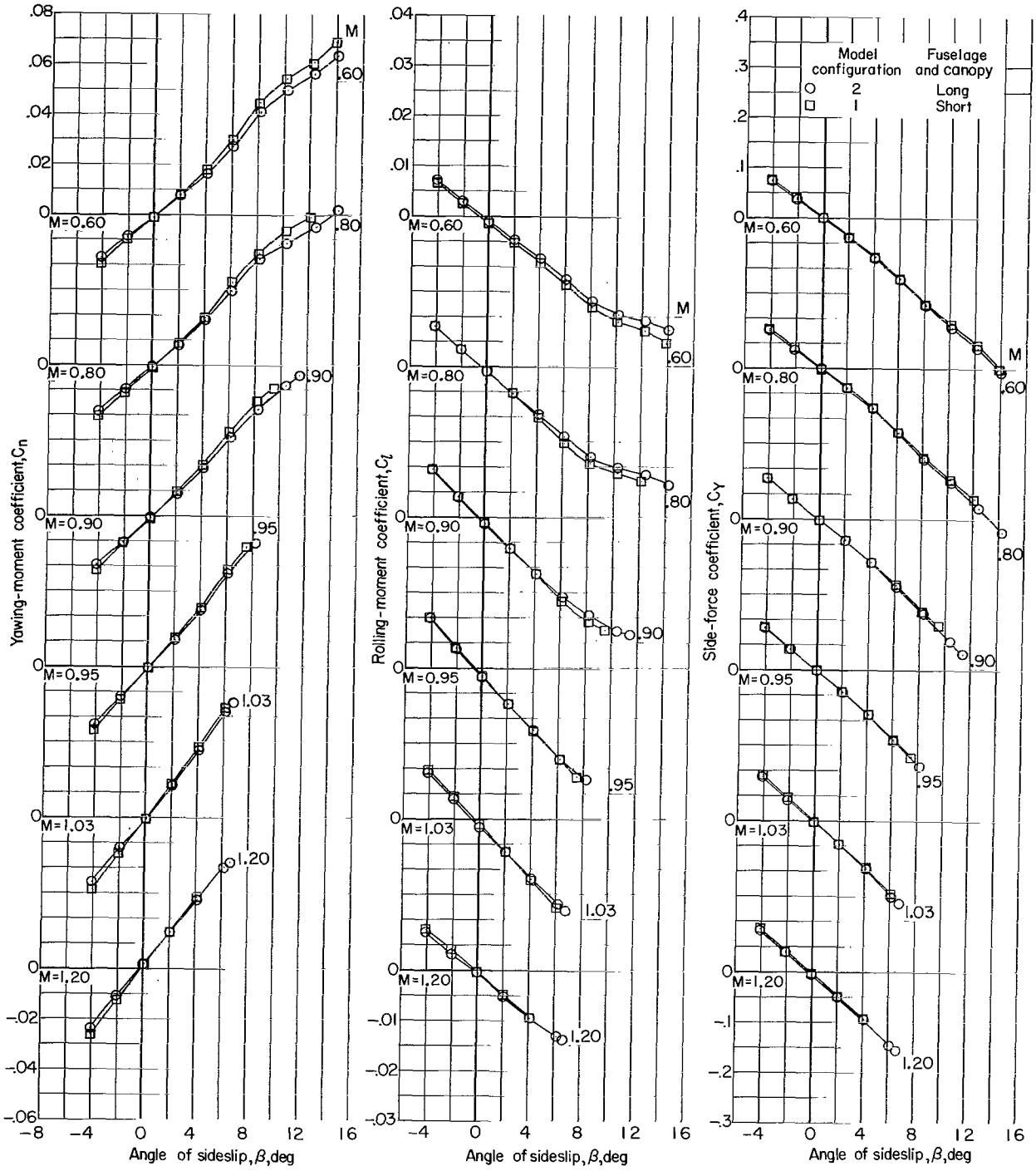

(a) $\alpha \approx 5.3^0$.

Figure 14.- Aerodynamic characteristics in sideslip of model configurations 1 and 2. $\delta_h = -3^0$.

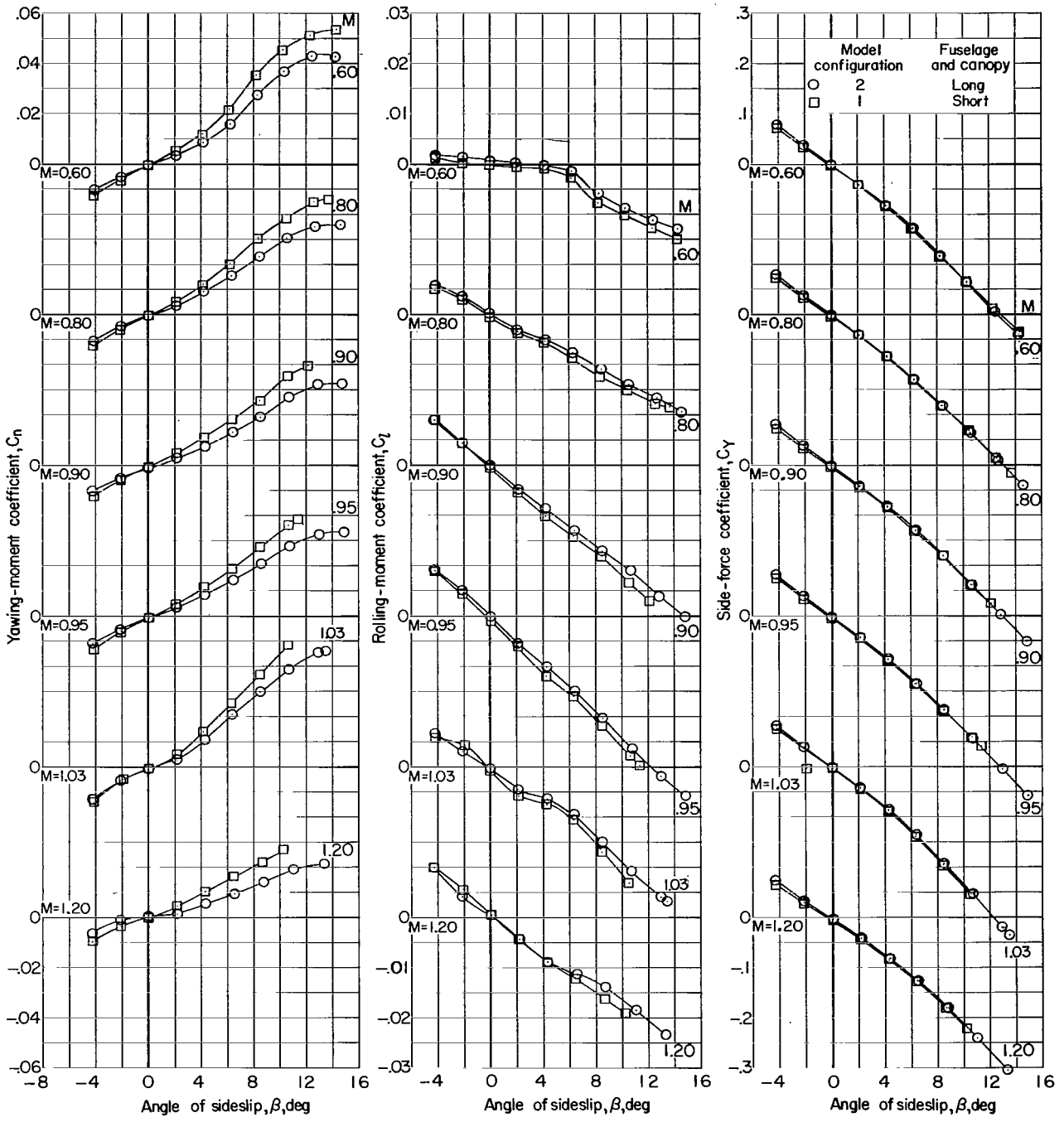

(b) $\alpha \approx 15.8^{0}$.

Figure 14.- Concluded.

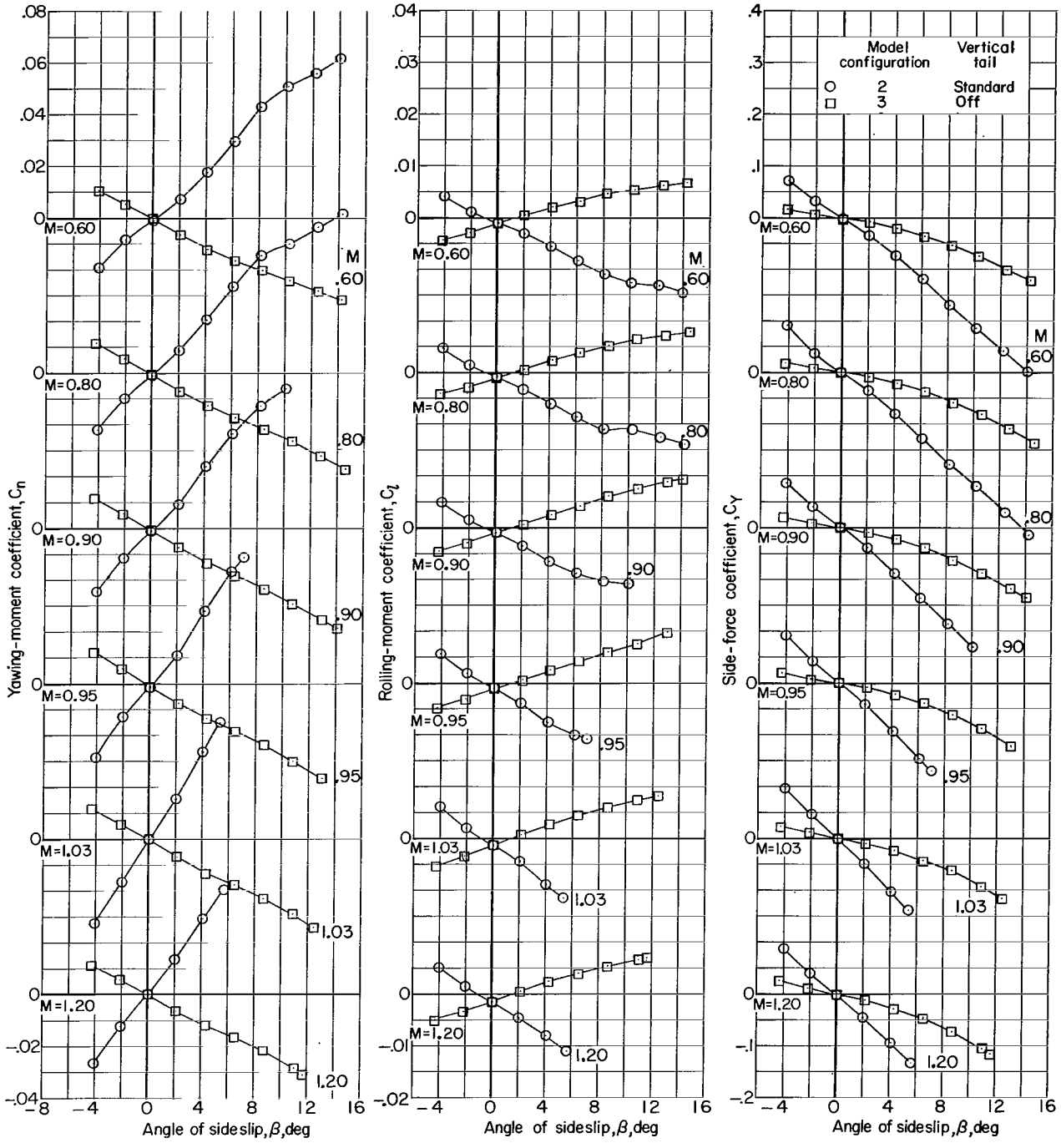

(a) $\alpha \approx 0^0$.

Figure 15.- Effect of vertical tail on aerodynamic characteristics in sideslip. $\delta_h = -3^0$.

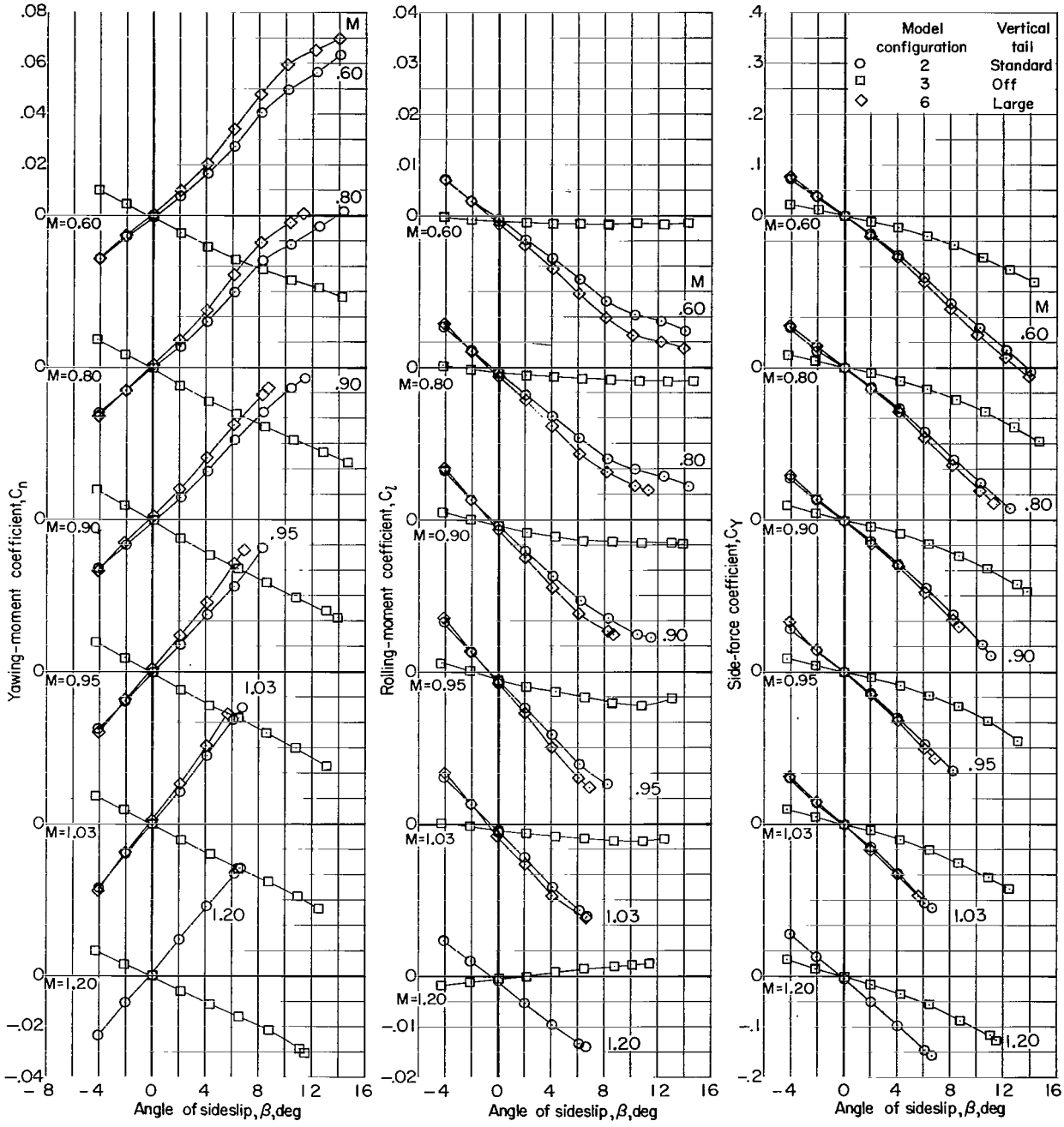

(b) $\alpha \approx 5.3^0$.

Figure 15.- Continued.

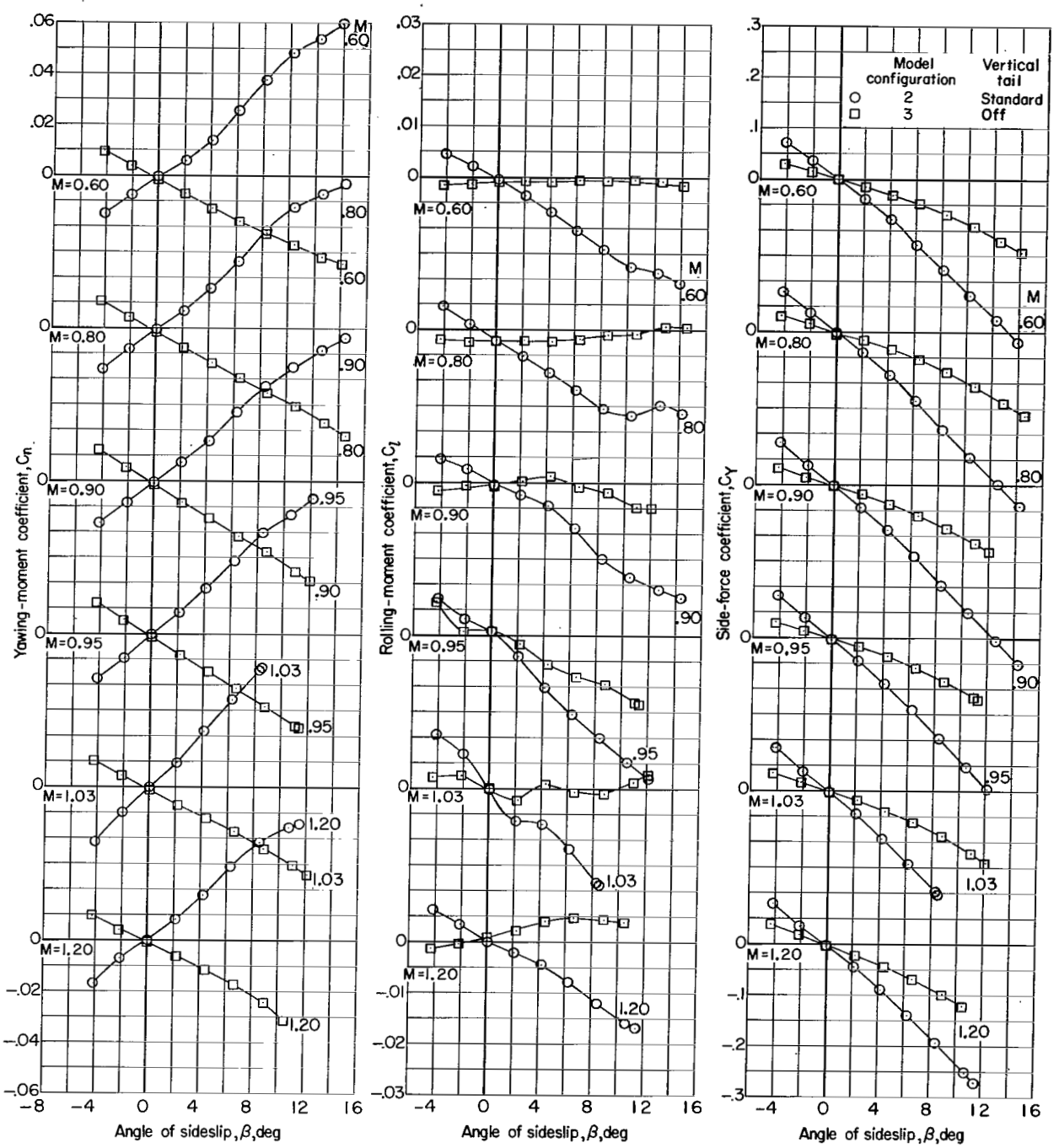

(c) $\alpha \approx 10.6^0$.

Figure 15.- Continued.

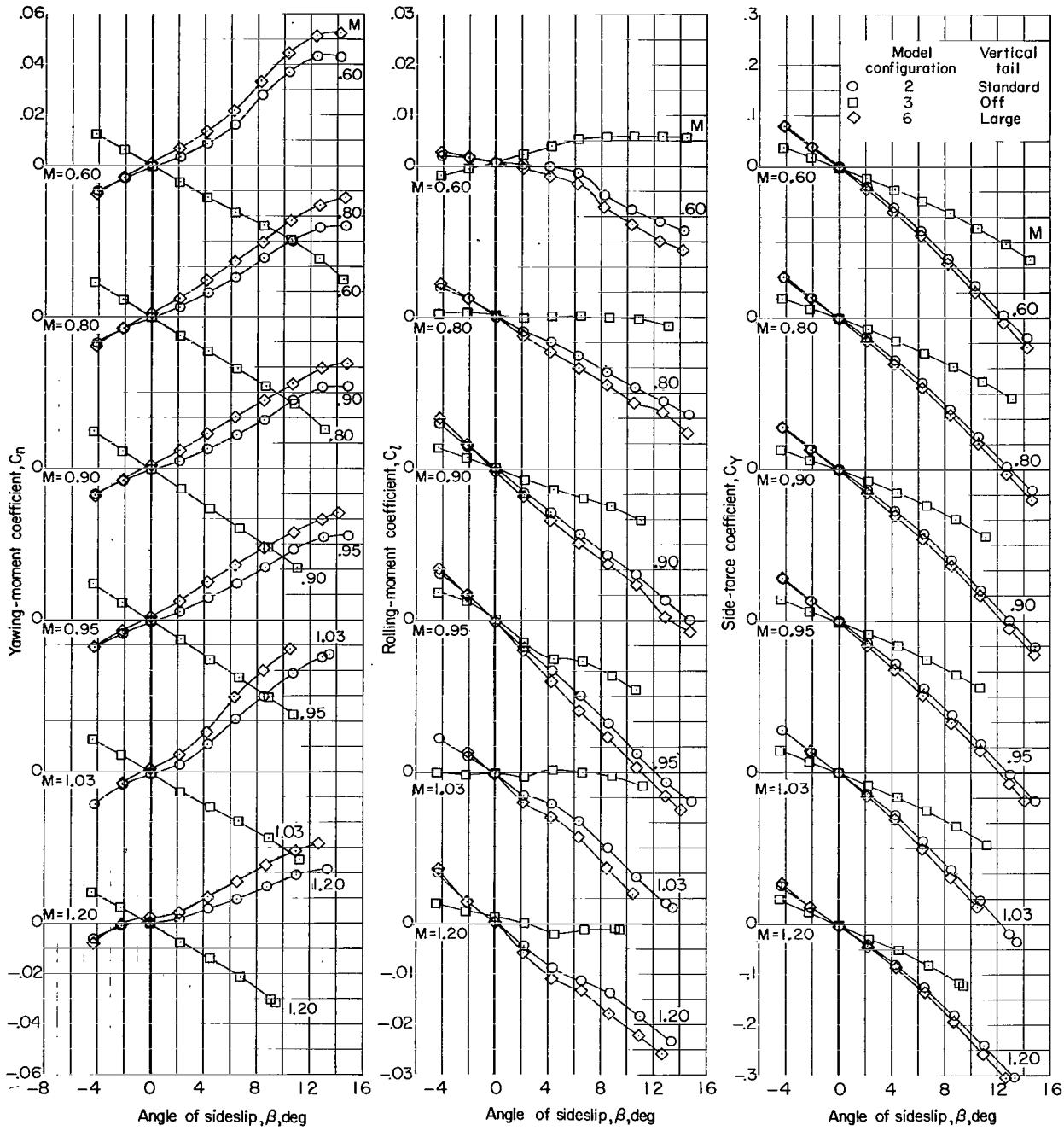

(d) $\alpha \approx 15.8^0$.

Figure 15.- Concluded.

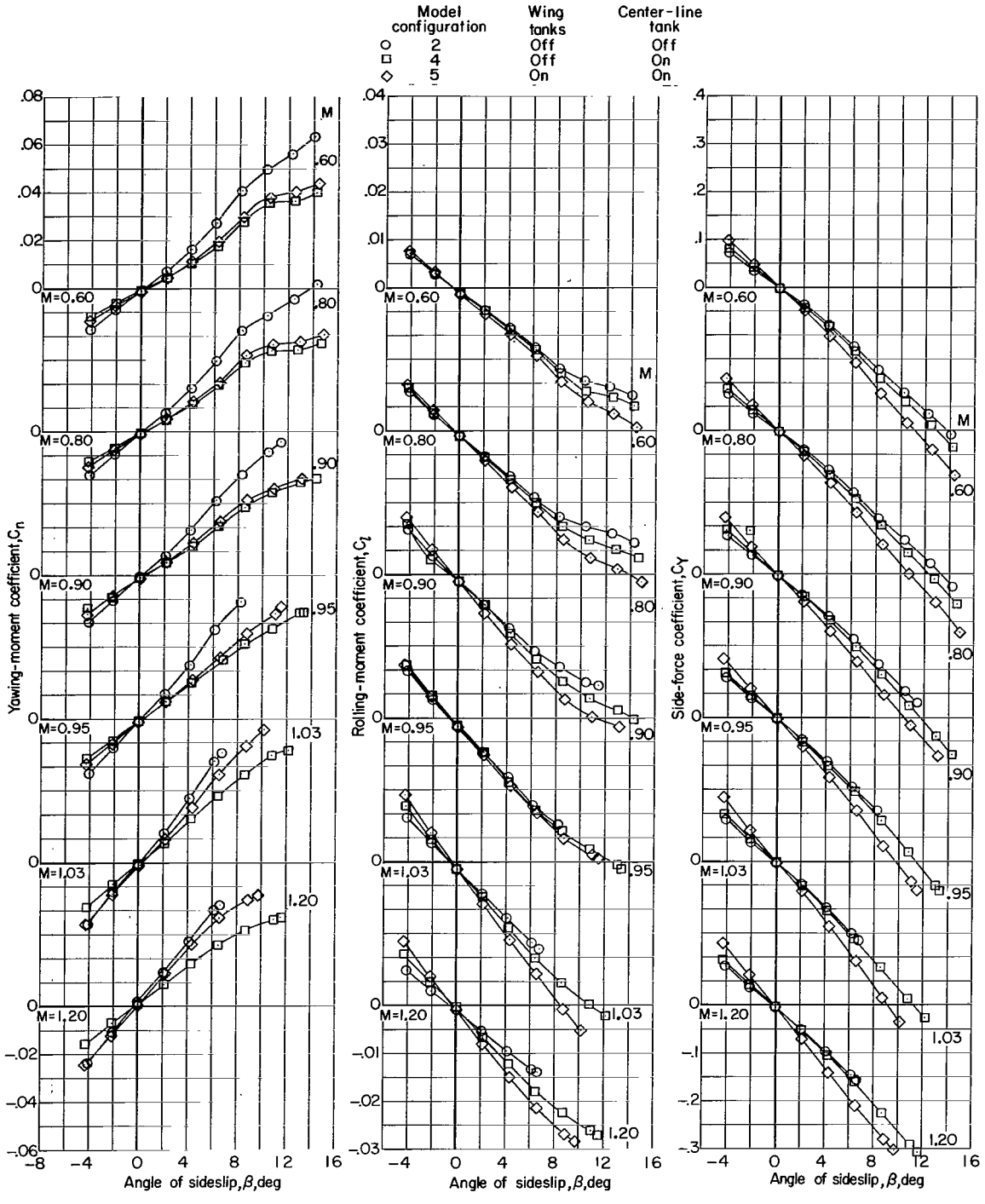

(a) $\alpha \approx 5.3^0$.

Figure 16.- Effect of center-line tank and wing inboard tanks on aerodynamic characteristics in sideslip. $\delta_h = -3^0$.

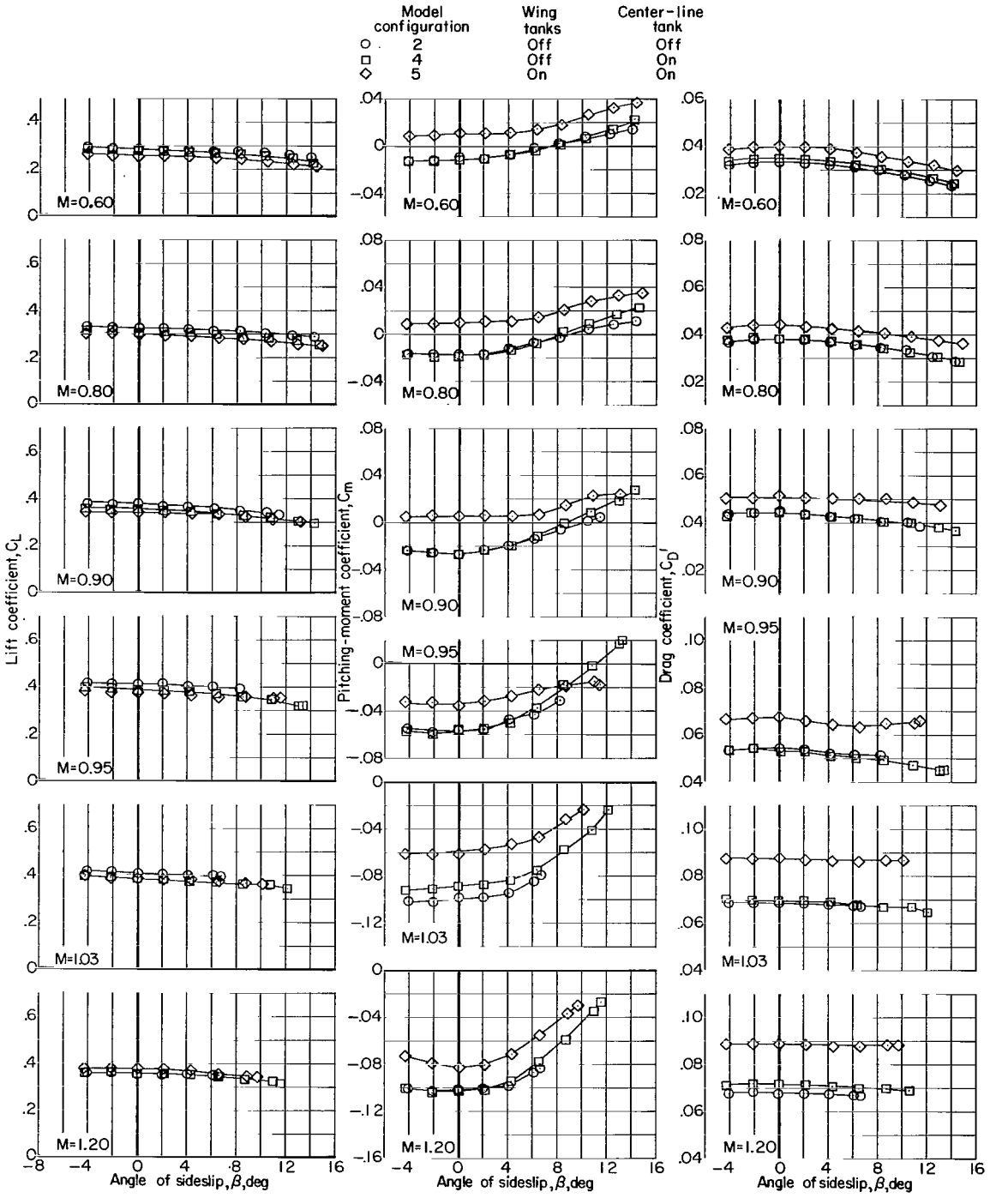

(a) $\alpha \approx 5.3^0$. Concluded.

Figure 16.- Continued.

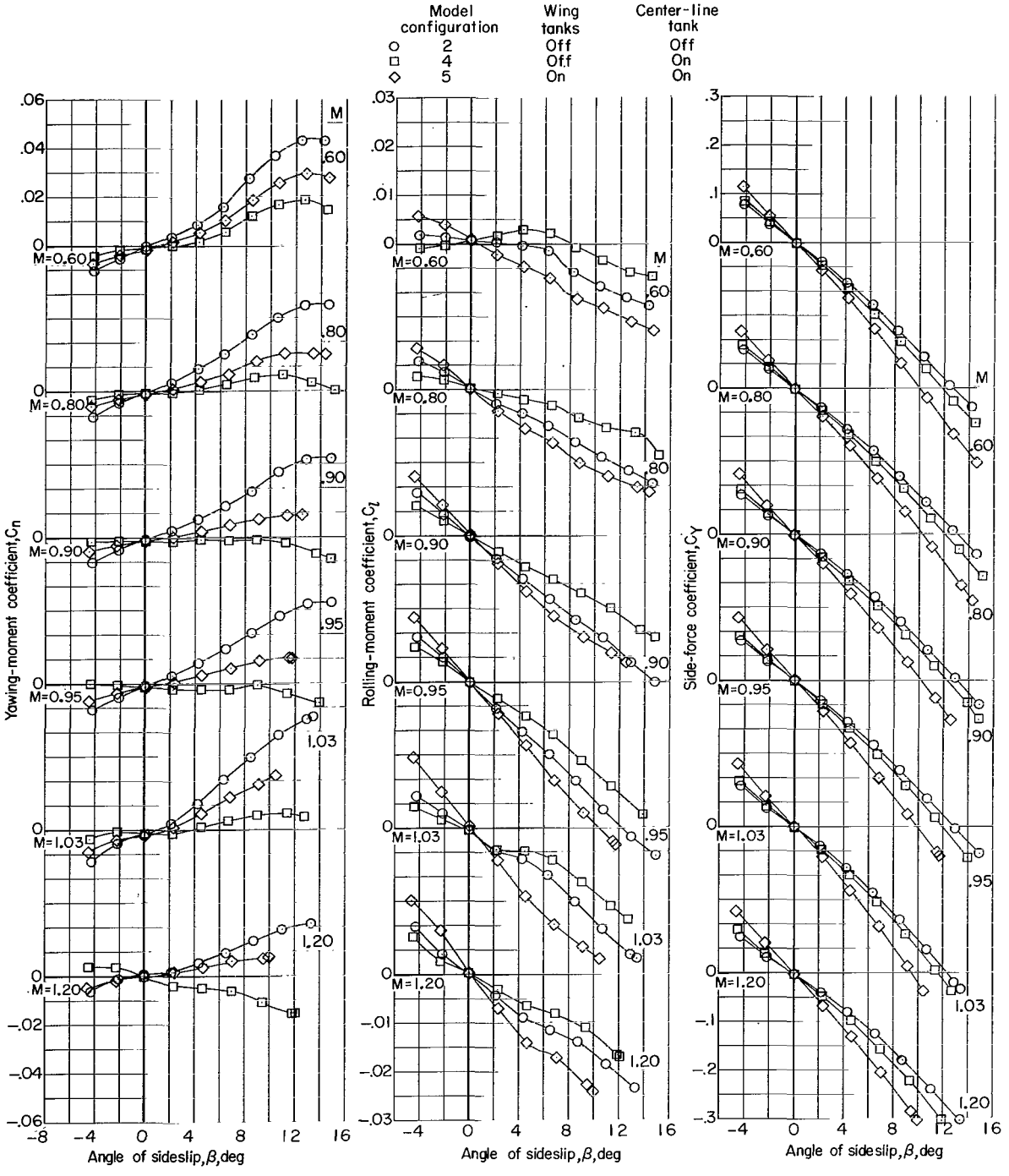

(b) $\alpha \approx 15.8^0$.

Figure 16.- Continued.

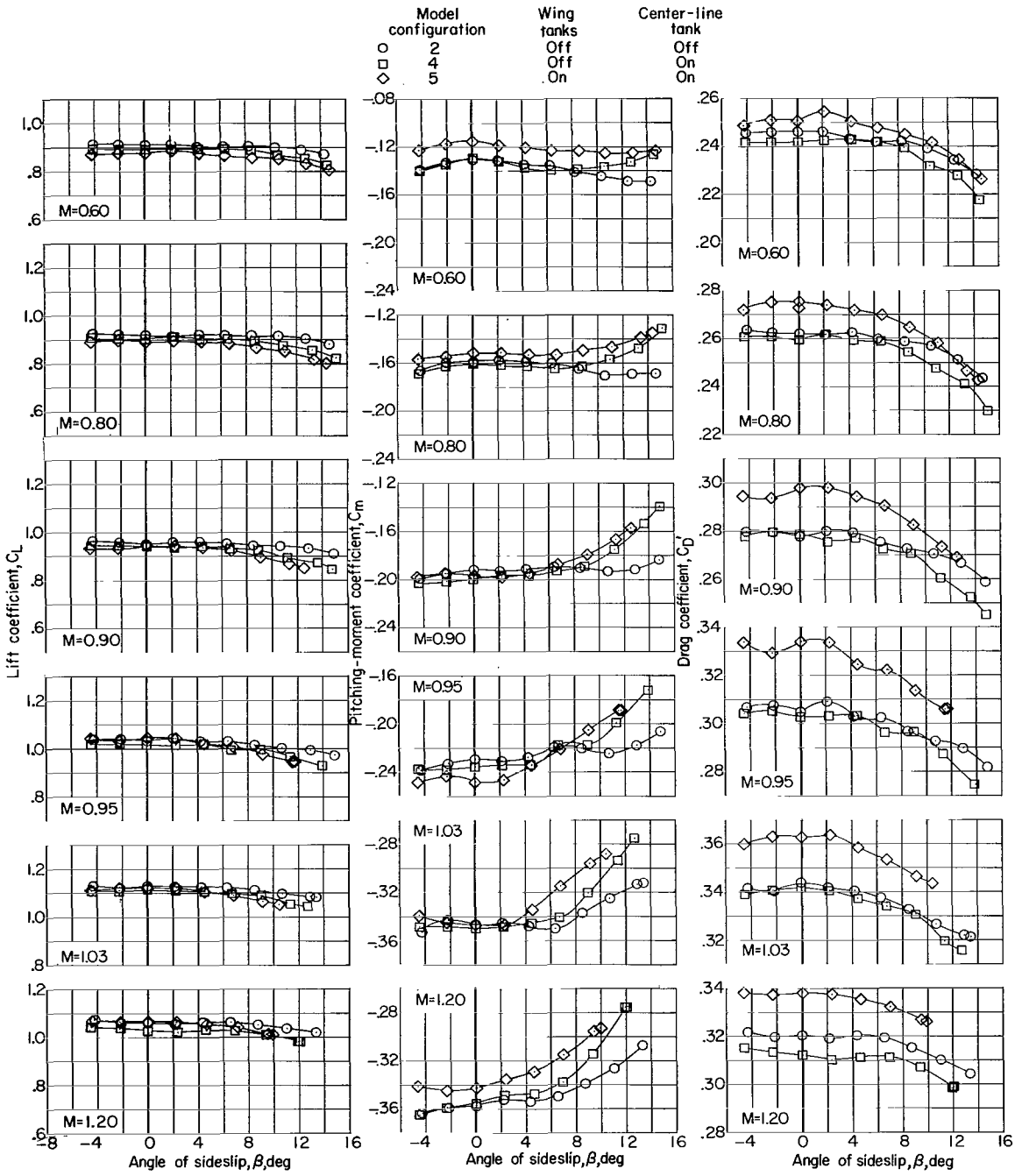

(b) $\alpha \approx 15.8$. Concluded.

Figure 16.- Concluded.

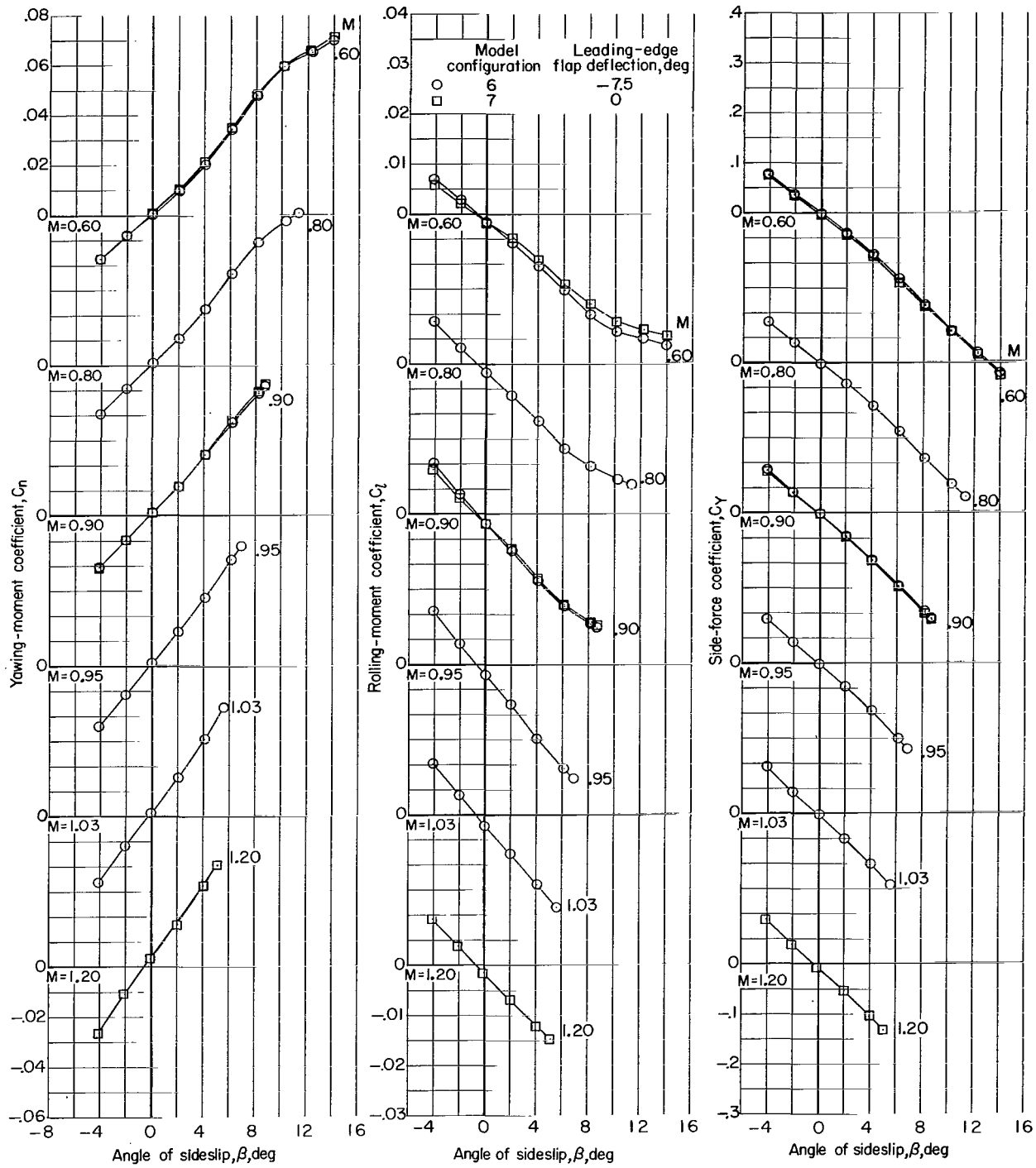

(a) $\alpha \approx 5.3^0$.

Figure 17.- Effect of deflection of leading-edge flaps on aerodynamic characteristics in sideslip. $\delta_h = -3^0$.

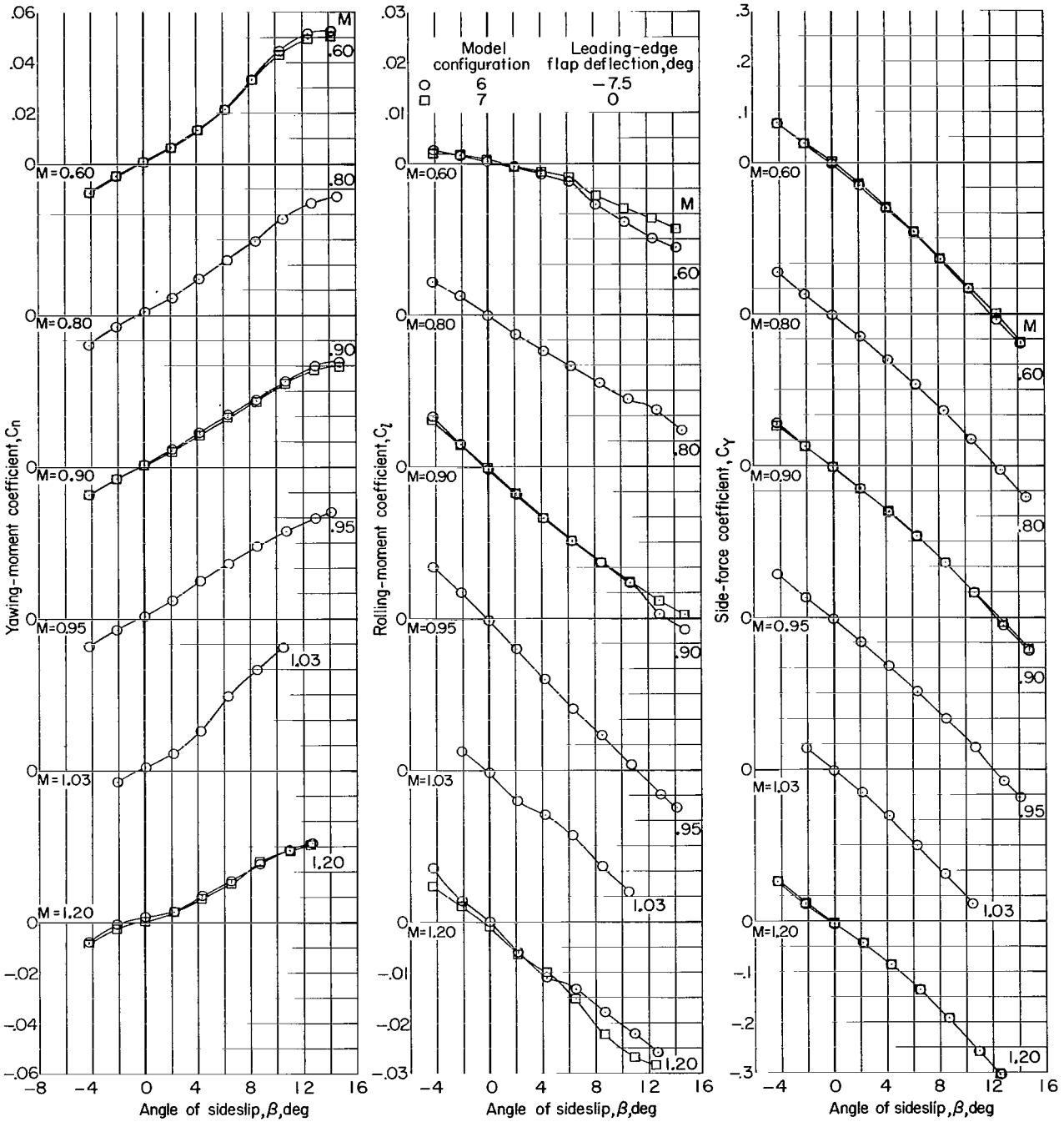

(b) $\alpha \approx 15.8^{0}$.

Figure 17.- Concluded.

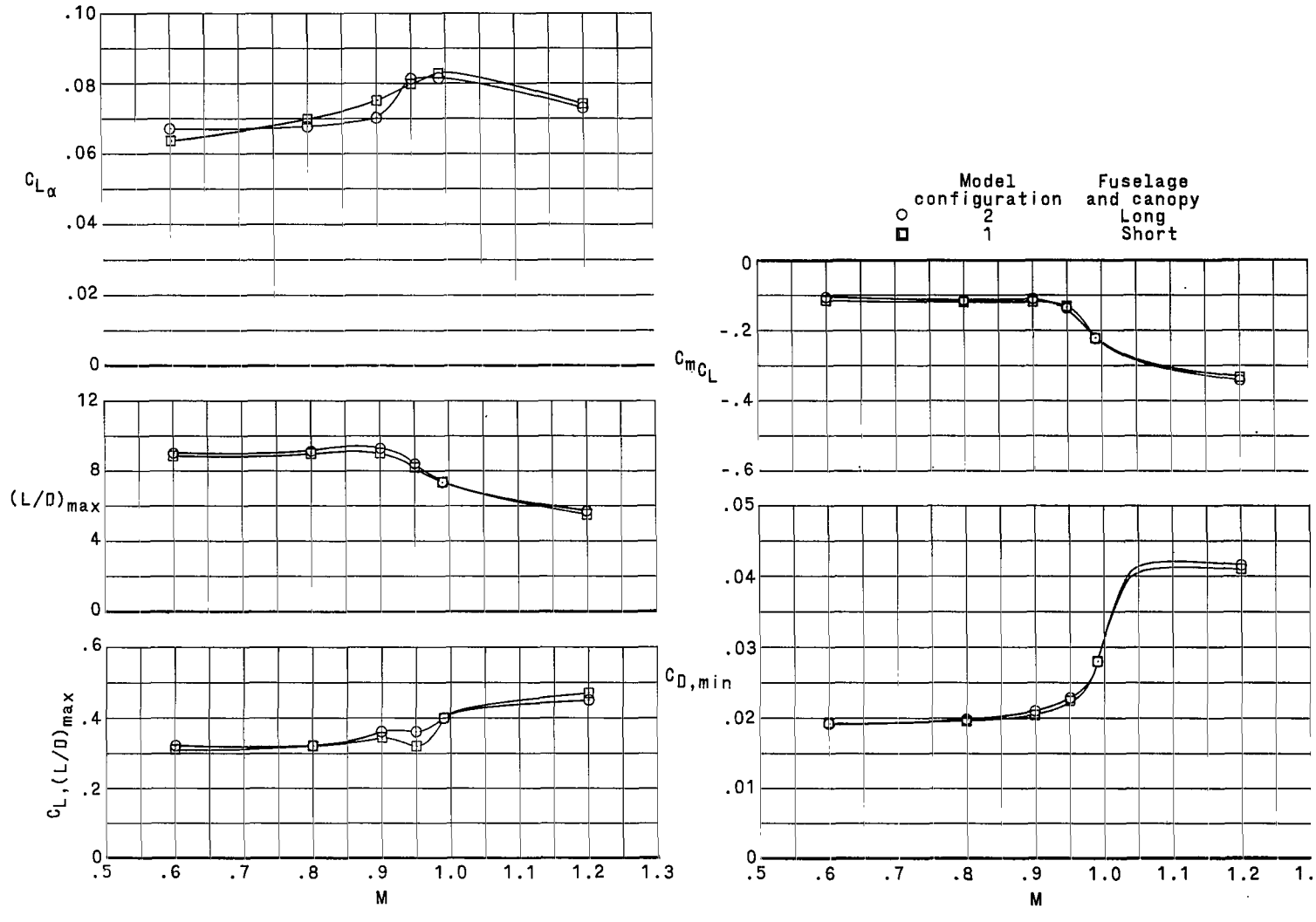

Figure 18.- Performance and longitudinal-stability derivatives of model configurations 1 and 2. $\delta_h = -3^0$; $\beta = 0^0$.

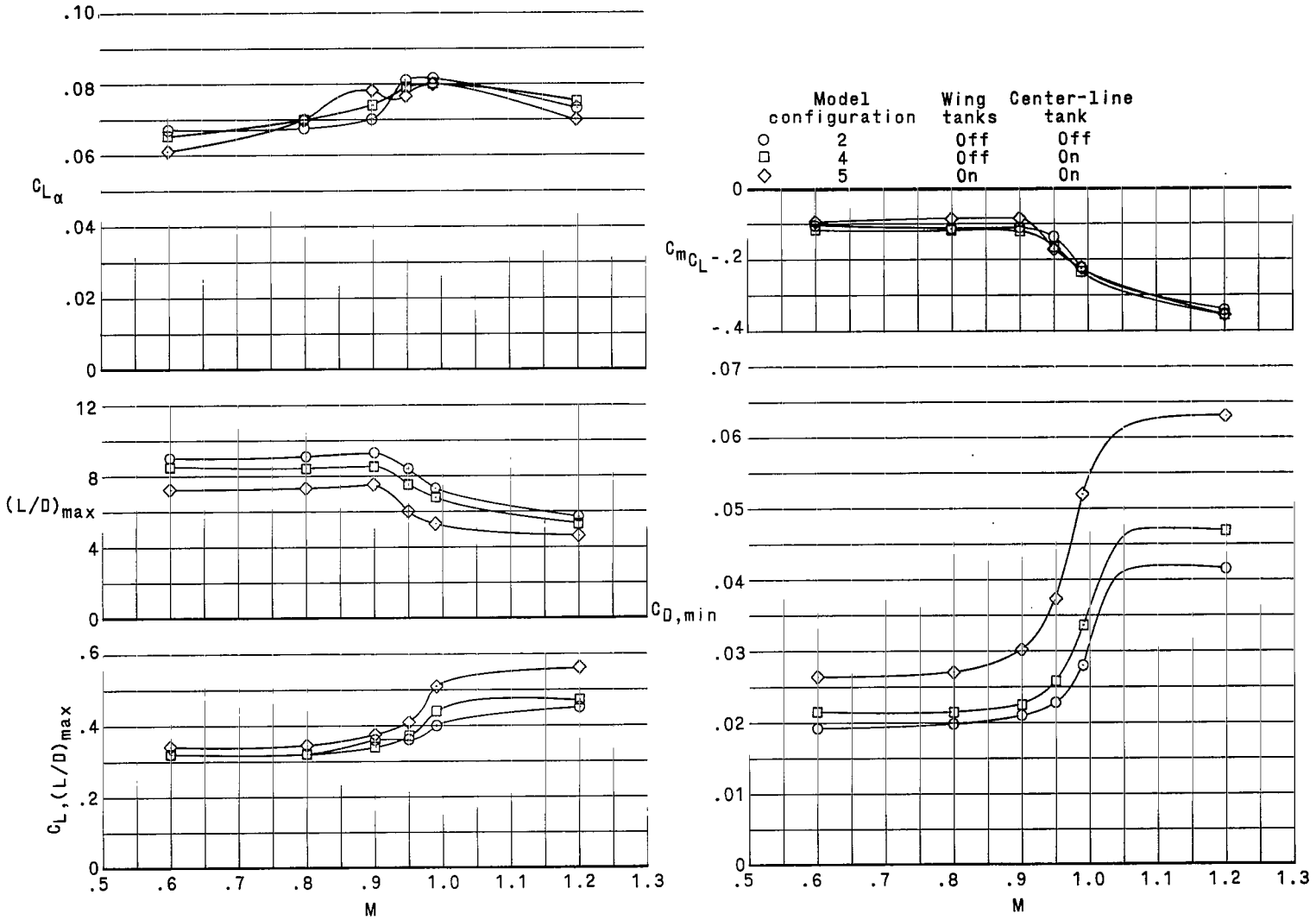

Figure 19.- Performance and longitudinal-stability derivatives of model configurations 2, 4, and 5. $\delta_h = -3^o$; $\beta = 0^o$.

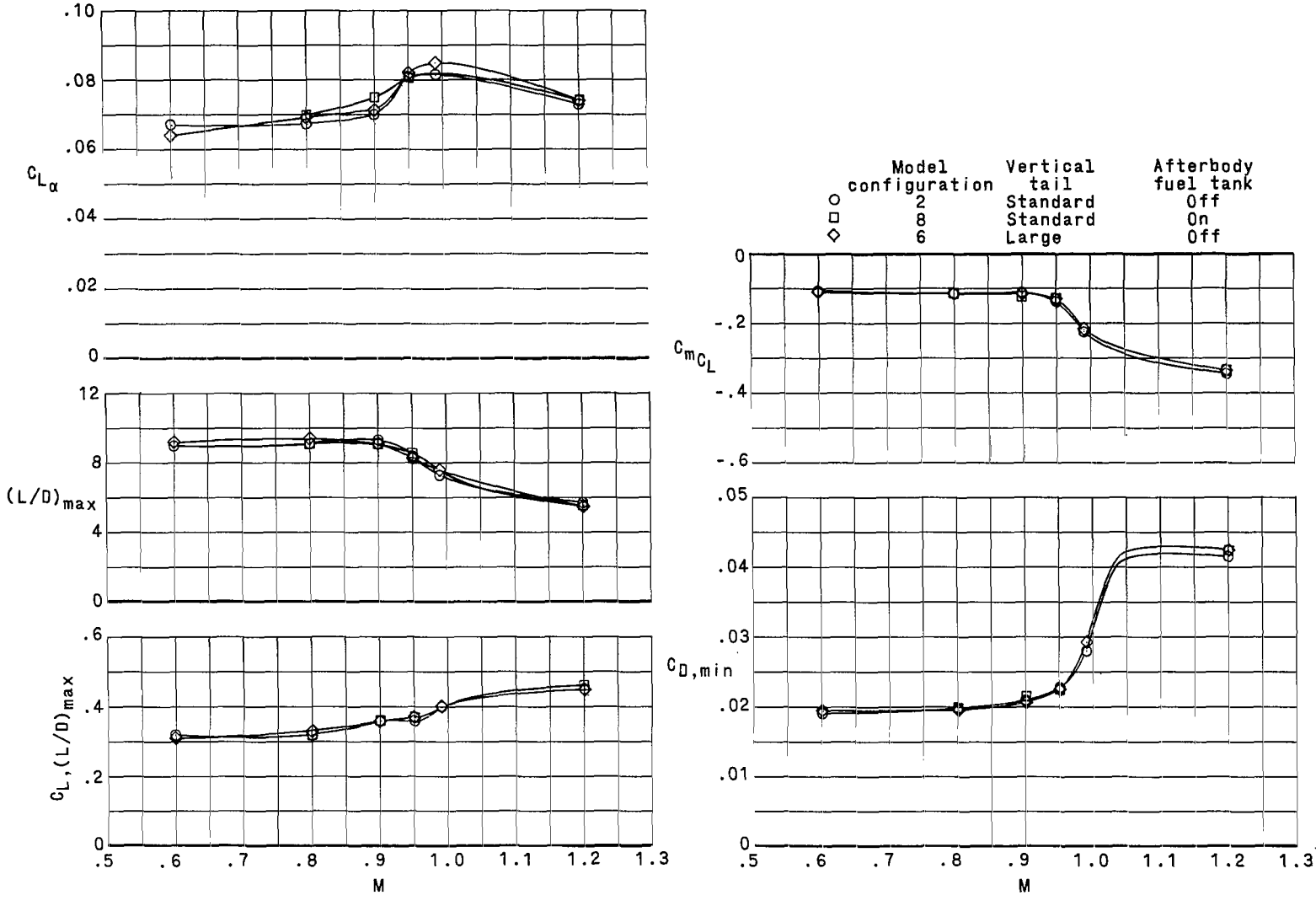

Figure 20.- Performance and longitudinal-stability derivatives of model configurations 2, 8, and 6. $\delta_h = -3^0$; $\beta = 0^0$.

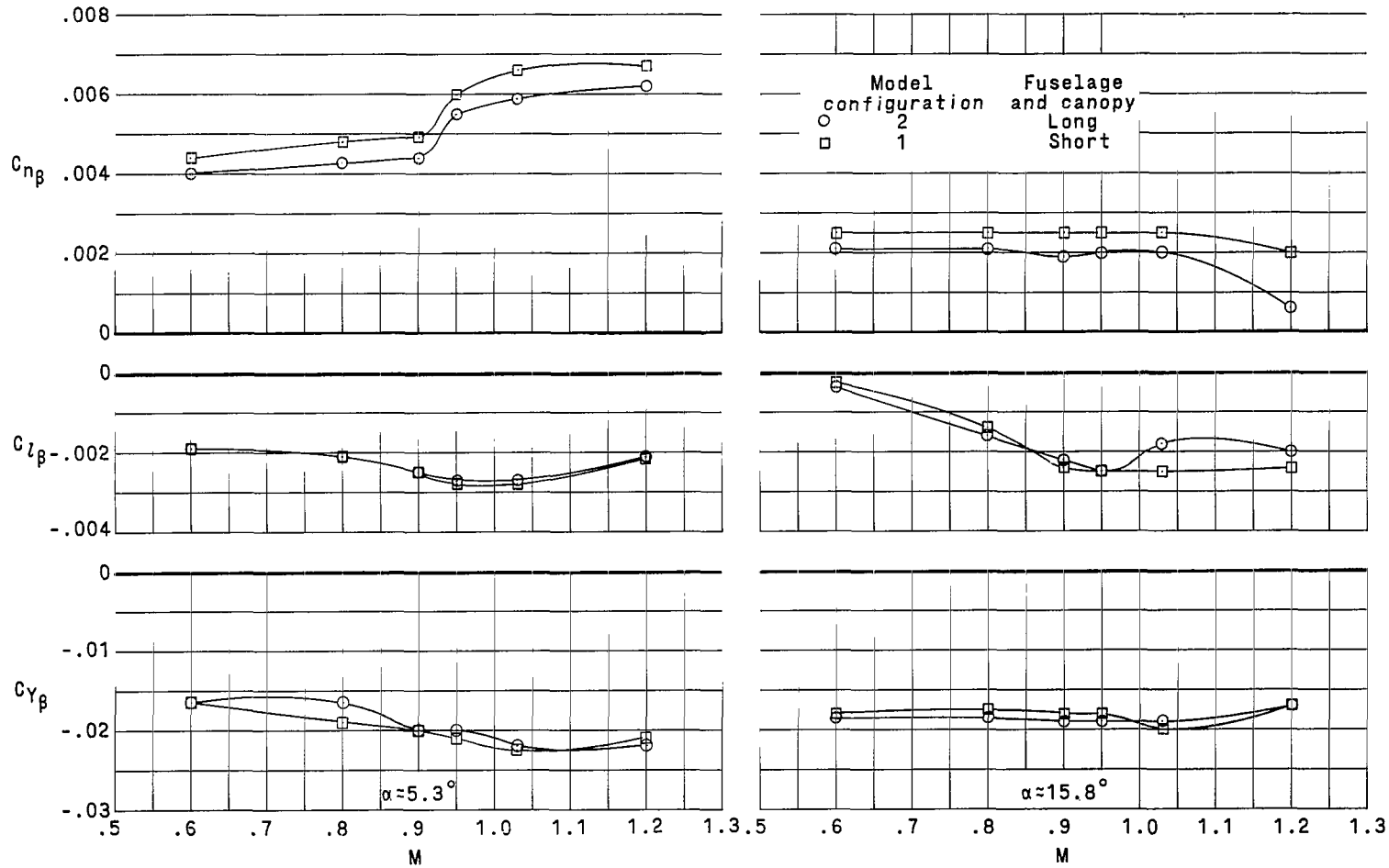

Figure 21.- Lateral-stability derivatives of model configurations 1 and 2. $\delta_h = -3^0$.

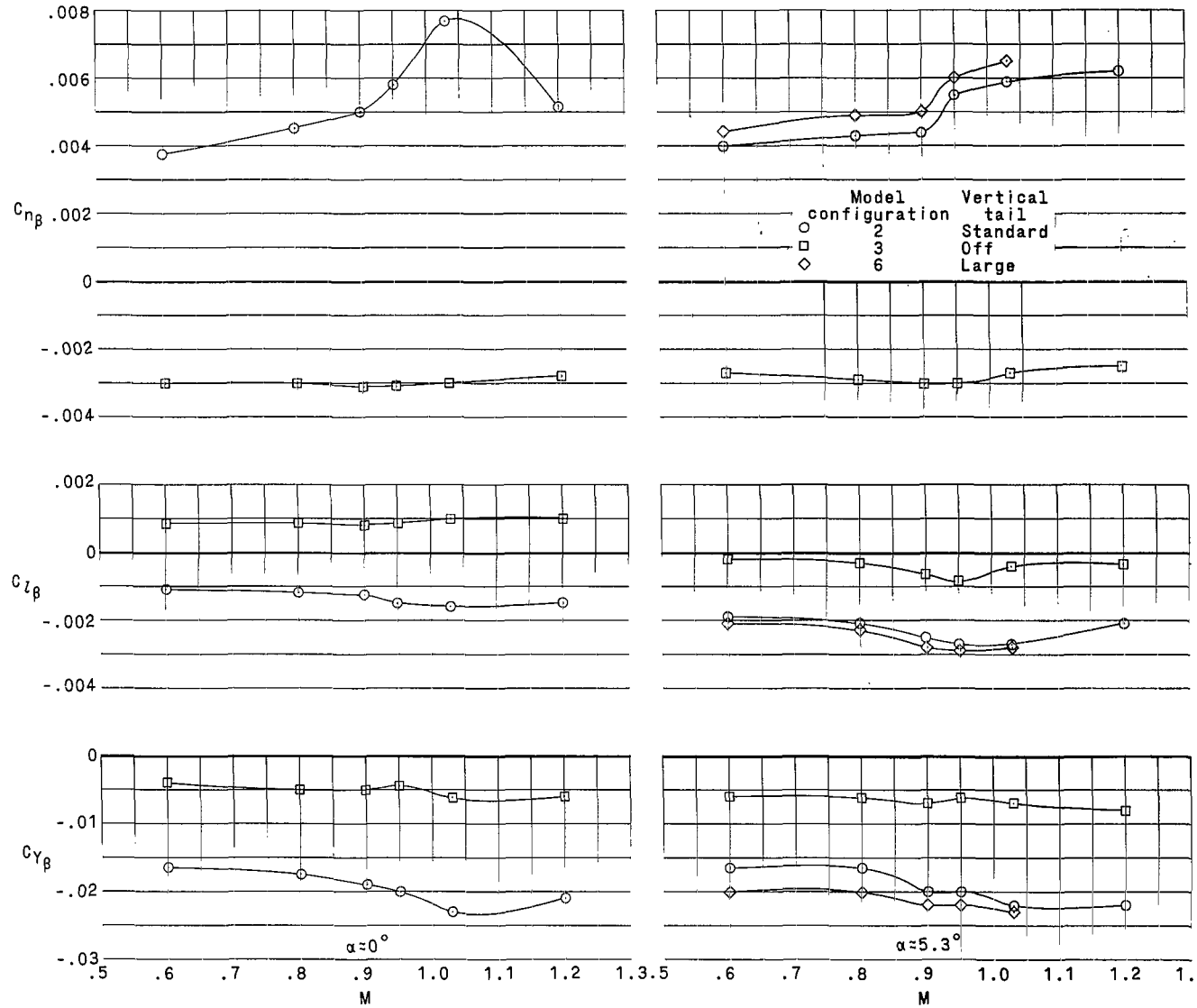

(a) $\alpha \approx 0^0$ and 5.3^0.

Figure 22.- Lateral-stability derivatives of model configurations 2, 3, and 6. $\delta_h = -3^0$.

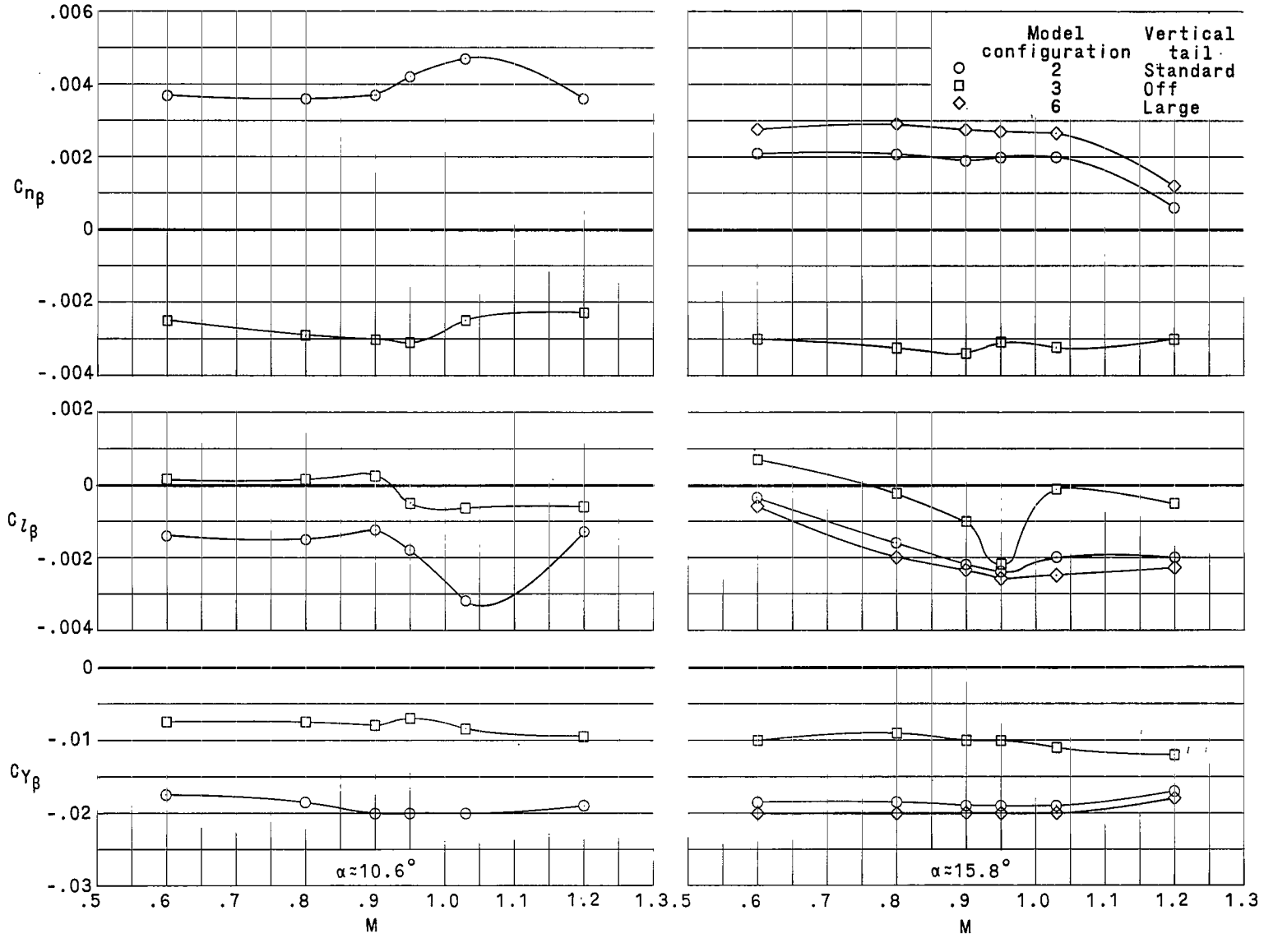

(b) $\alpha \approx 10.6^0$ and 15.8^0.

Figure 22.- Concluded.

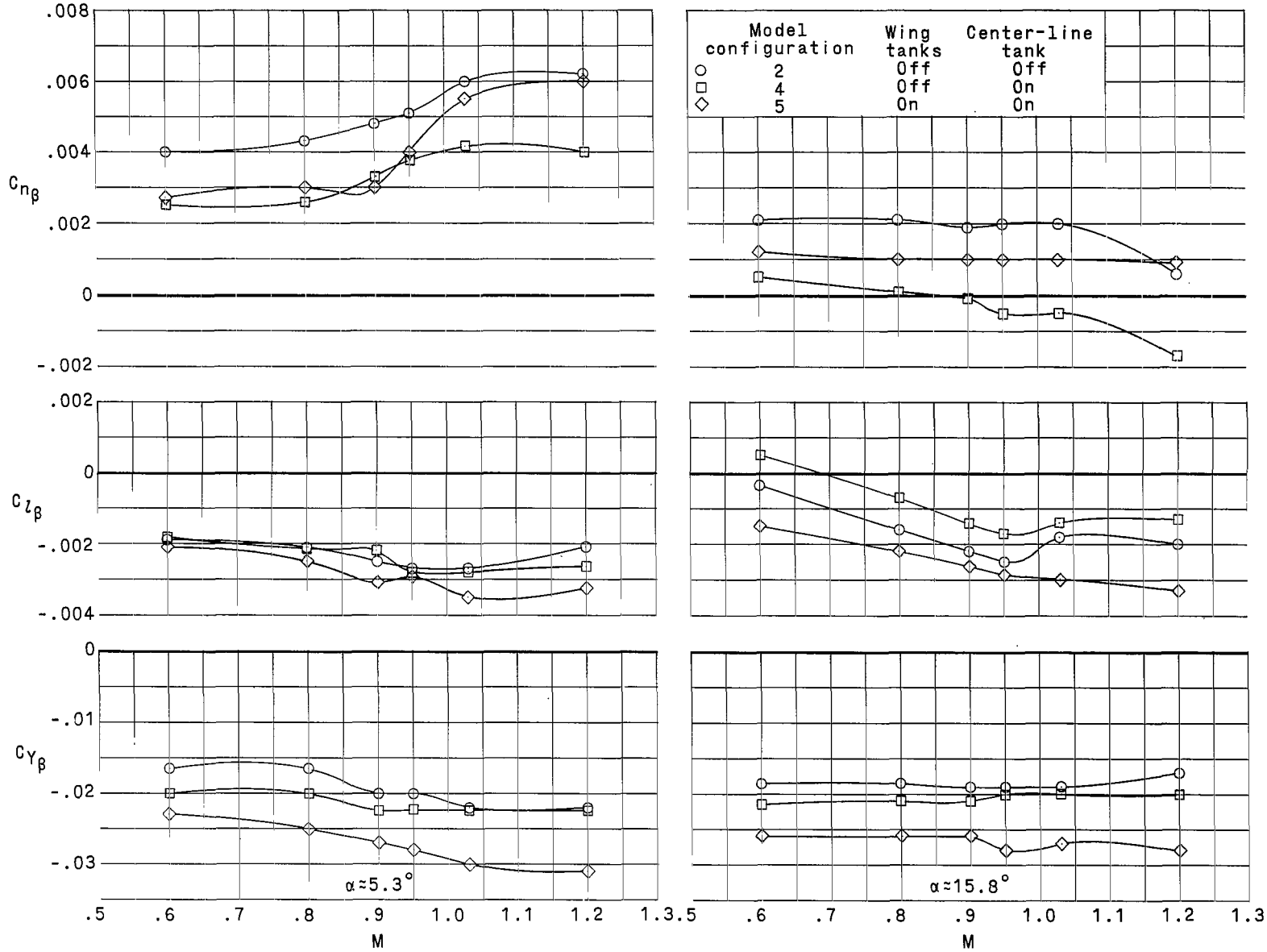

Figure 23.- Lateral-stability derivatives of model configurations 2, 4, and 5. $\delta_h = -3^0$.

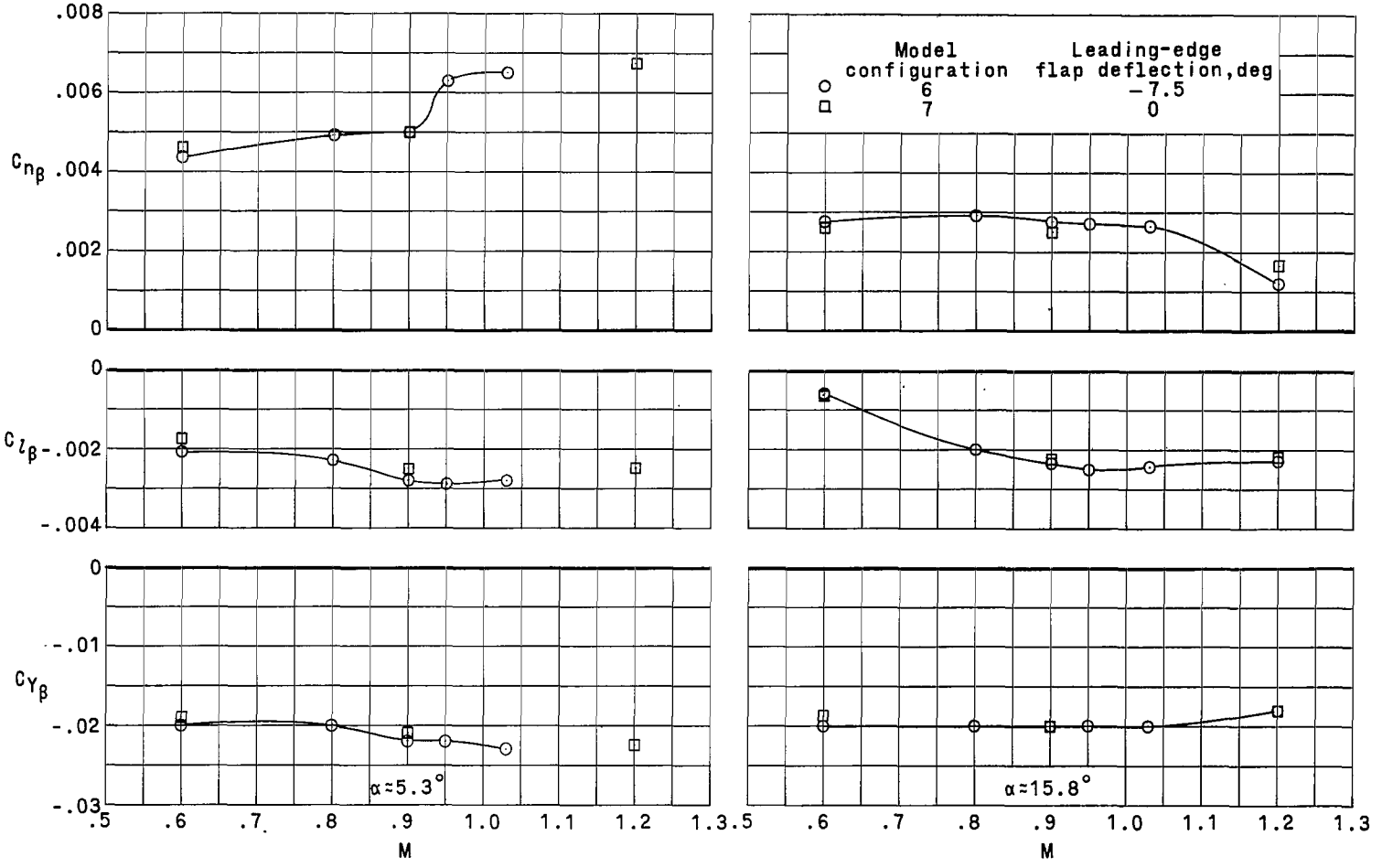

Figure 24.- Lateral-stability derivatives of model configurations 6 and 7. $\delta_h = -3^0$.

"The aeronautical and space activities of the United States shall be conducted so as to contribute . . . to the expansion of human knowledge of phenomena in the atmosphere and space. The Administration shall provide for the widest practicable and appropriate dissemination of information concerning its activities and the results thereof."

—NATIONAL AERONAUTICS AND SPACE ACT OF 1958

NASA SCIENTIFIC AND TECHNICAL PUBLICATIONS

TECHNICAL REPORTS: Scientific and technical information considered important, complete, and a lasting contribution to existing knowledge.

TECHNICAL NOTES: Information less broad in scope but nevertheless of importance as a contribution to existing knowledge.

TECHNICAL MEMORANDUMS: Information receiving limited distribution because of preliminary data, security classification, or other reasons.

CONTRACTOR REPORTS: Technical information generated in connection with a NASA contract or grant and released under NASA auspices.

TECHNICAL TRANSLATIONS: Information published in a foreign language considered to merit NASA distribution in English.

TECHNICAL REPRINTS: Information derived from NASA activities and initially published in the form of journal articles.

SPECIAL PUBLICATIONS: Information derived from or of value to NASA activities but not necessarily reporting the results of individual NASA-programmed scientific efforts. Publications include conference proceedings, monographs, data compilations, handbooks, sourcebooks, and special bibliographies.

Details on the availability of these publications may be obtained from:

SCIENTIFIC AND TECHNICAL INFORMATION DIVISION

NATIONAL AERONAUTICS AND SPACE ADMINISTRATION

Washington, D.C. 20546